

**NMR STUDIES
OF SHORT SALT BRIDGED PEPTIDES**

By

James A. Ernst

Submitted in Partial fulfillment
of the requirements for
Honors in the Department of Chemistry

UNION COLLEGE

June, 1994

ABSTRACT

ERNST, JAMES NMR Study of Small Salt Bridged Peptides.
Department of Chemistry, June, 1994.

The study of small helical peptides is an area of great interest in biochemistry. Baldwin has shown that salt bridging between residues with oppositely charged side chains can act to stabilize short helices. The order of increased helix stabilization shown by Baldwin was $i+4AB > i+4BA > i+3AB > i+3BA$ where A is a positively charged amino acid side chain and B is a negatively charged amino acid side chain.

Most previous studies have dealt with a single type of salt bridge stabilization, either $i,i+3$, or $i,i+4$ in a single peptide. This study will address the question of helix stabilization in a system of combined salt bridging. To this end a peptide was synthesized with $i,i+3$, $i,i+4$, $i,i+3$ spacing of oppositely charged residue side chain. The sequence of this peptide is: Ac-YEAAKAAEAAKAAEAAK-NH₂ (designated EK3.3). NMR study of this peptide is being carried out on a 500 MHz instrument. The proton spectrum is being assigned and the conformation determined through the use of TOCSY and NOESY experiments.

A second NMR investigation of the 5-mer Ac-YEAAK-NH₂ was carried out on a 200MHz instrument. This peptide is designed to allow study of structural stabilization in very small peptides through ionic interaction. The utility of various experiments including standard 1-D ¹H spectrum, and 2D COSY, DQF-COSY, Relayed COSY and NOESY on a 200MHz instrument is evaluated.

Acknowledgements

I wish gratefully thank the following people and institutions without whose help this would not have been possible.

Andrew and Nancy Ernst
My parents. Thanks always for their constant love and support.

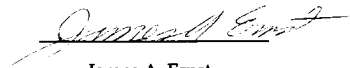
Professor Lesile Hull
His guidance and encouragement will always be appreciated.

Andy C. Wang, Ph.D
Whose patients and knowledge was indispensable.

Jay S. Berger
My always helpful partner in crime and research.

Union College

New York University



James A. Ernst

<u>Table of Contents</u>	<u>Page</u>
Chapter 1 Introduction	1
Characterization of Protein Structure	2
Helix Structures	5
Salt Bridging	6
Research Objectives	9
Experimnetal Measures of Helicity	10
Chapter 2 Experimental	15
Materials	16
Synthesis	17
Deprotection	19
Coupling	19
Capping	21
Cleavage	22
Analytical	25
HPLC	25
UV-Absorption	26
NMR	26
Mass Spectra	27
Chapter 3 Results and Discussion	28
Peptide Synthesis and Purification	29
Computer Modeling	30
NMR Study of the 5-Mer Peptides	33
Mathematical Resolution and	
Sensitivity Enhancement	33
Resolution and Sensitivity Enhancing functions	33
Shimming	36
Temperature	37
Spinning	37
Assignments of chemical shift	37
Two Dimensional Expariments	39
J-Resolved	29
COSY	39
DQF-COSY	41
Relayed COSY	43
Assignment of Coupling and Torsion Angles	47
Reduction of Peak Intesities	47
Water Suppression	49
The Nuclear Overhauser Effect	50
NMR Study of the 18-mer Peptides	51
TOCSY	52
NOESY	53
DQF-COSY	53

<u>Table of Contence continue</u>	<u>Page</u>
Chapter 4 Conclusion and Future Research	56
Computer Modeling	57
5-Mer NMR Studies	57
Future Research	58
18-Mer NMR Studies	59
Future Research	60
Other Futer Studies	60
References	62
Appendix 1 Computer Modeling	69
1.1 MacroModel .com File For The Model EK4.0 Peptide	70
1.2 MacroModel Output File for the Model EK4.0 Peptide	71
1.3.1 The Lowest Energy Model of the EK 4.0 Peptide	73
1.3.2 The Lowest Energy Model of the EK 4.0 Peptide	74
1.4.1 The Lowest Energy Model of the EK 3.3 Peptide	75
1.4.2 The Lowest Energy Model of the EK 3.3 Peptide	76
Appendix 2 Resolution Enhancement	77
2.1 ^1H 1-D Spectrum of EK5, No Enhancement	78
2.2 ^1H 1-D Spectrum of EK5, With 32K Zero Fill	79
2.3 ^1H 1-D Spectrum of EK5, With Line Narrowing, Lorentzian-Gaussian Transformation and Zero Fill	80
Appendix 3 NMR Spectra of the 5-Mer Peptides	81
3.1 KE5 ^1H 1-D Spectrum at pD 2.9	82
3.2 KE5 ^1H COSY at pD2.9	83
3.3 EK5 ^1H 1-D Spectrum at pD 2.9	84
3.4 EK5 ^1H 1-D Spectrum at pD 7.0	85
3.5 EK5 ^1H 1-D Spectrum at pD 11.0	86
3.6 EK5 ^1H J- Resolved pD 7.0	87
3.7 EK5 ^1H 1-D Spectrum at pD 7.0 500MHz	88
3.8 EK5 ^1H COSY pD3	89
3.9.1 EK5 ^1H DQF-COSY pD 7.0 Non-spinning Sample	90
3.9.2 EK5 ^1H DQF-COSY pD 7.0 Expanded Region Non-spinning Sample	91
3.10 EK5 ^1H Relayed COSY pD 7.0 $\tau = 35\text{ms}$	92
3.11.1 EK5 ^1H DQF-COSY pD 11.3, Non-spinning Sample	93
3.11.2 EK5 ^1H DQF-COSY pD 11.3, Spinning Sample	94
3.12 EK5 NOESY pD 2.9 200 ms mixing time	95

Table of Contents continued

	<u>Page</u>
Appendix 4 NMR Studies of the 18-mer Peptide	96
4.1 EK4.0 ¹ H 1-D Spectrum at pH 5.5 500 MHz	97
4.2.1 EK3.3 ¹ H 1-D Spectrum at pH 5.5 500 MHz	98
4.2.2 EK3.3 ¹ H 1-D Spectrum at pH 5.5 200MHz	99
4.3 EK4.0 TOCSY pH5.5	100
4.4 EK4.0 NOESY pH5.5 200 ms mixing time	101
4.5 EK3.3 TOCSY pH5.5	102
4.6 EK3.3 NOESY pH5.5 200 ms mixing time	103
4.7.1 EK3.3 DQF-COSY pD 7.0 200MHz	104
4.7.2 EK3.3 DQF-COSY pD 7.0 200MHz Expanded Regions	105

Table of Figures

	<u>Page</u>
1.1 Amino Acids, Names Abbreviations and One Letter Codes	3
1.2 Peptide Nomenclature	4
2.1 AMA Rink Amide Resin	16
2.2 Reaction Flask	18
2.3 Fmoc cleavage	19
2.4 Coupling Pathways	20
2.5 Peptide Coupling	22
2.6 Setup for Vacuum Filtration of Cleavage Mixture	23
2.7 TFA Side Chain Protecting Group Cleavage	24
2.8 TFA Resin Cleavage	25
3.1 FID Zero Fill	34
3.2 Application of a Window Function	35
3.3 Pulse Sequences	55

Table of Tables

	<u>Page</u>
1.2 Structural Parameters of α and 3_{10} Helices	6
2.1 Protocol for Peptide Synthesis	18
3.1 Weight and Yield of Peptide Synthesis	29
3.2 Proton Assignments of the KE5 Peptide in ppm	38
3.3.1 EK5 pD 2.9 Proton Assignments	44
3.3.2 EK5 pD 7.0 Proton Assignments	44
3.3.3 EK5 pD 11.3 Proton Assignments	45

Chapter 1

Introduction

Globular proteins exhibit complex topology. The structure of proteins is determined by the order of amino acids and the environment in which the protein exists. The basic forces which govern protein folding have been known for many years, but their interactions are highly complex and a detailed understanding of how these forces shape protein folding is not yet available. This research intends to further elucidate some of the interactions which stabilize protein folding. Thus this study addresses some of the interactions present in small helical peptides which act as models for similar structures in globular proteins. Further knowledge in this area will contribute to a better knowledge of forces stabilizing helices in globular proteins.

CHARACTERIZATION OF PROTEIN STRUCTURE

There are four orders of protein structure. The primary structure is the connectivities of different amino acids. For the purposes of this study it is convenient to group the commonly occurring amino acids into five categories:

Amino acids with hydroxyl or sulfur containing side chains: serine, cysteine, threonine and methionine.

Aliphatic amino acids: alanine, valine, leucine, isoleucine, proline and glycine.

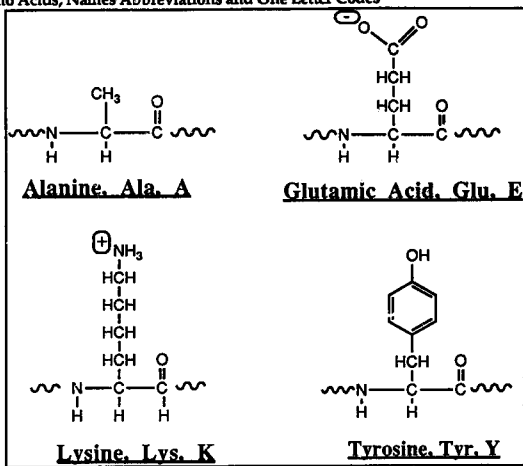
Basic amino acids: lysine, histidine and arginine.

Acidic amino acids and their amides: aspartic acid, glutamic acid, asparagine, and glutamine.

Aromatic amino acids: tyrosine, phenylalanine and tryptophan.

Four of the twenty commonly occurring amino acids are of particular interest to this study. Their structures, names, abbreviations and one letter codes are presented in Figure 1.1.

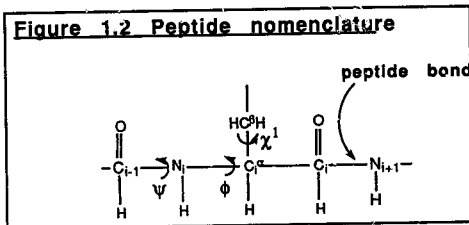
Figure 1.1 Amino Acids, Names Abbreviations and One Letter Codes



The formation of peptide bonds between amino acids creates what is known as the peptide backbone. Residues, the amino acid sub-units in proteins and peptides, are typically numbered sequentially beginning at the amino terminus (also known as the N-terminus). Residues of particular interest are designated *i*. Residues with which the *i* residue interacts may be designated by numbering from the *i* residue ¹.

Individual atoms in residues may be designated using Greek letters or their Roman equivalents (See Figure 1.2 for illustration). It is also useful to define certain angles of rotation in the peptide backbone in order to discuss peptide orientation. Rotation about the N^{*i*} to C_{*i*}^α bond (C_{*i-1*}, N_{*i*}, C_{*i*}^α, C_{*i*}) is defined as the φ angle. Rotation about the C_{*i*}^α to C_{*i*} bond (N_{*i*}, C_{*i*}^α, C_{*i*}, N_{*i+1*}) is defined as ψ. Rotation about the C_{*i*} to N_{*i+1*} bond (C_{*i*}, C_{*i*}, N_{*i+1*}, C_{*i+1*}^α) is defined as ω. The eclipsed conformation is given the value 0. Values are given from

-180 to +180 with positive rotation being dextrorotary rotation of A looking down the bond A,B,C,D¹. For discussion purposes ω is typically neglected as it is limited to approximately 0 or 180 due to the double bond character between the carbonyl group and nitrogen.



The secondary structure in proteins and peptides is the organization of certain domains of amino acid chains into one of a few common repeating sub-units. Early studies in the 1950s by Linus Pauling identified two common repeating secondary structures in globular proteins². These structures are denoted α -helices and β -pleated sheets. The defining characteristics of these structures is the orientation of hydrogen bonds between amide hydrogens and carbonyl oxygens. Sections of proteins which do not exhibit any explicit structure are said to be in a random coil conformation, although this is not generally considered a secondary structural unit. A denatured protein is considered to be in a 100% random coil conformation.

The overall topology of the folding of the secondary structure is known as protein tertiary structure. Proteins may also exhibit quaternary structure which is the aggregation of several protein sub-units into a single structure, such as the aggregation of the four separate peptide chains ($\alpha_2\beta_2$) in hemoglobin.

Helix Structures

In α -helix structures there is hydrogen bond formation between carbonyl oxygens and amide protons of one residue designated i and a residue four amino acids away designated $i+4$. It has been noted that the α -helix is the most common secondary structural unit in the native structure of globular proteins³, additionally it is a common early intermediate in protein folding⁴. These two features make the helices a particularly interesting object for further research.

The highly complex nature of protein structure, outlined above, makes it difficult to study many of the factors influencing secondary structure as it exists in the native protein. Fortunately it is possible to synthesize artificial peptides to simulate many of the factors affecting secondary structure and subsequently to pursue a detailed study of secondary structures in a limited, controlled environment.

There are a variety of helices which can occur in globular proteins. Theoretically helices may adopt both left handed (clockwise) and right-handed (counterclockwise) orientations. However, the discussion of helical structures here is limited to right handed helices as left-handed helices are almost unknown in natural proteins. The structure of a helix may be characterized in several ways. The number of repeating sub-units (amino acids) per turn is n . The rise in the helix per residue is d . The product of these two measurements is p , the pitch of the helix ($p=nd$). Pitch is the distance parallel to the helix traveled per complete turn of the helix. For the α -helix $n=3.61$ residues $d=1.50\text{\AA}$ and $p=5.41$.

A second kind of helix, the 3_{10} helix, of particular interest in small peptides. This is a tighter helix than the α -helix with hydrogen bonding between the amide proton and the carbonyl oxygen of i to $i+3$ residues. A comparison of some parameters of helicity for α and 3_{10} helix are given in Table 1.1.

Increasing peptide length is known to favor increased helicity. It has also been shown that increasing peptide length in alanine based peptides favors α -helix formation over 3_{10} helix formation. Additionally, what 3_{10} helix does exist in such peptides is seen to co-exist with the α -helix in the C-terminus of longer peptides as opposed to than the N-terminus of shorter peptides⁵.

Table 1.1 Structural Parameters of α and 3_{10} - Helices

	α -helix	3_{10} helix
ϕ	-48°	-49°
ψ	-57°	-26°
n (residues)	3.61	3.00
d (Å)	1.50	2.00
p(Å)	5.41	6.00

From reference 6

SALT BRIDGING

The average α -helix in globular proteins is only 11 residues⁷, thus small peptides are of particular interest in helix study. However, in early research the study of helix formation in small peptides presented some difficulties and long synthetic peptides were the system of choice in studying peptide helix formation⁸. Studies of these peptides led to Zimm-Bragg helix coil transition theory. In this theory, host guest experiments on random co-

polymers of amino acids provided numeric values for nucleation of the helix (σ) and propagation of the helix (s), for the twenty common amino acids. Calculation based on these values and the Zimm-Bragg equation predicted that peptides shorter than 20 amino acids would show no helix formation at any temperature^{7b}. However, two peptides derived from ribonuclease, C-peptide (residues 1-13) and S-peptide (residues 1-20) show measurable helix formation at 1°C⁷. This suggests a mechanism of helix formation which is not addressed by Zimm-Bragg.

Thus it was necessary to pursue other explanations for the helix stabilization of short peptides. X-ray crystallographic studies of C-peptide and the S-peptide showed close interaction between the negatively charged Glu2 residue and the positively charged Arg10. It was postulated that these two residues form a salt bridge (ion pairing) which stabilizes helix formation. Direct study of salt bridge induced helix formation in the S-peptide and C-peptide proved difficult. This led to de novo peptide design to study helix formation.

Robert Baldwin proposed several model peptides to study salt bridge induced helix formation. In these models Baldwin spaced positively and negatively charged amino acids at i to $i+3$ and i to $i+4$ locations in the peptide. Baldwin hypothesized that since the α -helix has 3.6 residues per helix turn, positively and negatively charged residue side chains at i to $i+3$ and i to $i+4$ locations in the peptide should provide special helix stabilization as this spacing would place the residues on the same side of the helix and hence in good location to form salt bridges. Further, alanine shows special helix formation propensity, therefore Baldwin chose it as the amino acid backbone of his peptides⁹. Peptides were synthesized with lysine and

glutamic acid interactions as this pair of oppositely charged amino acids have been found to show the large helix stabilization¹⁰. Baldwin eventually arrived at four model systems⁷.

KE i,i+4 Ac-AKAAAEEKAAAEEKAAAEEA-NH₂ 17-mer

EK i,i+4 Ac-AEAAAKEAAAKEAAAKA-NH₂

KE i,i+3 Ac-AKAAEEKAAEEKAAEEA-NH₂ 16-mer

EK i,i+3 Ac-AEAAKAEAAKAEAAKA-NH₂

The EK i, i+4 peptide shows the greatest helix stabilization of these four peptides. This peptide shows 80% helicity at 10°C and significant helicity is seen even at 70°C. The i to i+3 peptides show the least helicity. In fact they show strikingly less helicity than the i, i+4 peptides. This is particularly interesting; both have oppositely charged amino acids on the same face of the helix and thus might be expected to show similar helicity. Baldwin was unable to explain experimentally why preferential helix stabilization is seen in the i,i+4 peptides. However, Baldwin theorized decreased stability in the KE peptides as compared with the EK peptides might be caused by an unfavorable interaction with the helix dipole in the KE peptides not present in the EK peptides⁷. The helix stabilization is greater in these peptides than in the in alanine mono-peptide or alanine, lysine or alanine glutamic acid co-peptides (e.g., (AAAK)_x or (AAAE)_x)¹².

By measuring helix concentration of the peptide at varied pH, Baldwin demonstrated that helix formation in the EK i,i+4 is due to salt bridging. His findings showed that helicity was increased at near neutral pH where lysine and glutamic acid are oppositely charged and therefore free to form salt bridges. Helicity in the EK i,i+4 peptide also showed substantial increased over the other model peptides at any pH. Baldwin hypothesized that this was due to hydrogen bonding between charged amino acids and uncharged

residue at the $i+4$ location. This theory was supported by studies at high ionic concentration (up to 5M) where ionic interactions would be completely shielded⁷.

RESEARCH OBJECTIVES

Current literature focuses on only a single type of salt bridging in a peptide. We propose that a study of helix formation in a hybrid of the $i,i+3$ and $i,i+4$ peptides may provide additional insight into the greatly enhanced helix formation in the $i, i+4$ peptide in relation to the $i,i+3$ peptide. To pursue this investigation four peptides were synthesized:

KE5= Ac-YKAAE-NH₂ 5-mer

EK5=Ac-YEAAK-NH₂

EK3.3 =Ac-YEAAKAAEAAAKAAEAAK-NH₂ 18-mer

EK4.0= Ac-YEAAAKAEAAAKAEAAK-NH₂

(analogous to Baldwin $i, i+4$ peptide)

The 5-mer peptides were synthesized to provide small systems suitable for 200MHz NMR studies which may provide further information on ionic interactions very small peptides.

The EK3.3 peptide contains: a section of $i,i+3$ EK opposite charge spacing, a section of $i,i+4$ EK opposite charge spacing and a second section of $i,i+3$ EK opposite charge spacing. The EK4 peptide is analogous to the Baldwin's EK $i,i+4$ peptide with two changes. First, alanine was inserted between K5 & E7 and K11 & E13 residues in order to make the EK4 and EK3.3 peptides the same length. It is noted that Baldwin's $i,i+3$ and $i,i+4$ peptides differ in length by one residue and it is wondered what role this may have played in increasing helicity in the longer $i,i+4$ peptide. Second, tyrosine was

added at the N-terminus to act as a chromophore for use in concentration studies and for identification in HPLC purification. (Tyrosine is a know helix de-stabilizer, however, it is hoped that by placing tyrosine at the end of the helix any de-stabilizing influences will be limited.) The synthesized peptides were also capped at the N-terminus by an acetyl group and at the C-terminus by an NH₂ group. This is done for several reasons: 1) to prevent further reaction at the terminus; 2) to limit unfavorable dipole interaction with the terminus which would otherwise be charged; 3) to add another peptide bond and thus increase helical tendencies⁹⁻¹⁰.

It will be a major focus of this research to investigate the use of a 200MHz NMR in determining the structure of a small 5-mer peptide and to evaluate the structures of the 18-mer peptides by NMR.

The peptides are synthesized manually using a solid phase 9-Fluorenylmethoxycarbonyl (Fmoc) synthesis as out lined in Jones¹³. The primary reason for use of the Fmoc method over the slightly more common BOC (t-Butoxycarbonyl) method is to avoid the hazardous and unpleasant hydrogen fluoride cleavage associated with BOC cleavage from the solid phase support. A more complete discussion of the Fmoc synthesis is available in the experimental section.

EXPERIMENTAL MEASURES OF HELICITY

A large number of experimental methods exists for studying helicity in peptides. Literature analysis reflects the following: Circular Dichroism (CD), Nuclear Magnetic Resonance (NMR), Electron Spin Resonance (ESR) and X-ray Crystallography.

CD is the method of determining helicity of peptides most commonly used. CD spectra of helical peptides show two characteristic minima at 222nm and 208nm and a maximum at 193nm. The theoretical $[\Theta]$ for a "100%" helix has estimated by extrapolation from data on helicity of a peptide at various concentrations of trifluoethanol (a known helix inducer). For the 222nm minima $[\Theta]_{222\text{nm}}$ for 100% helix has been determined as $-36000\text{deg}\cdot\text{cm}^2/\text{dmol}$. By comparing experimental intensity at 222 nm to the theoretical minima for 100% helicity it is possible to determine percent helicity.

CD is a relatively quick and simple method of determining overall peptide helicity. It is also highly sensitive compared with other methods of determining helicity. Measurements are typically taken in the area from 5-100 μM . This makes CD an excellent method for determination of concentration, pH and temperature dependence of helicity. It is also typical to take spectrum at various concentrations of a denaturing agent (e.g., guanidine chloride) to provide reference spectrum of the random coil peptide and the helix-coil transition⁷.

While CD is a very powerful method of determining overall helicity it provides no information of the detailed structure of the helix. For such information we must turn to other methods. X-ray crystallography has long been the method of choice for studying the detailed structure of proteins and peptides. It is not, however, a simple technique.

ESR is largely analogous to NMR, the major differences in the spectrum are due the fact ESR has greatly increased sensitivity relative to NMR and many artifacts not seen in NMR experiments are seen in the ESR

spectrum. In the study of peptides it is necessary to provide spin labeled compounds for ESR. Caution must be taken to see that these compounds do not effect the structure of the peptide. Discussion and example of ESR in the study of helical peptides may be found in reference 5.

NMR is extensively used to provide detailed information on the structure of peptide and it is widely used in the literature^{7,14,15}. The method provides three basic sources of experimental information on peptide structure. First, torsion angles for peptides may be determined from three bond coupling constants of $^3J_{\text{NH-H}\alpha}$ and $^3J_{\text{H}\alpha,\text{H}\beta}$ and the empirically derived Karplus equations for the ϕ and χ^1 angles^{15,16}. Such assignments can usually be made from a Double Quantum Filtered COSY (DQF-COSY)¹⁷. Second, distance information in peptides may be derived from the use of the Nuclear Overhauser Effect (NOE) measurements. NOEs can be obtained from 2D NOESY experiments and arise from through space coupling of nuclear dipoles. NOEs can provide information about spatial orientation of atoms at a distance of up to 4.5-5Å^{15,18}. Short range NOEs are most useful for determining the sequence of amino acids through amide proton to amide proton coupling. Longer range NOEs can provide nearly 100% confirmation of helicity in peptides. Individual NH, $i,i+3$ (for 3_{10} helix) and $i,i+4$ (for α -helix) NOEs are approximately 80% unique for each helical structure. The existence of several of these NOE interactions can be taken as confirmation of 3_{10} or α -helix^{15,19}.

Confirmation of helix structure in peptides may be further constrained by the use of build up NOE's. This is done by varying the mixing time in the NOESY experiment. This can provide approximate information on the maximum distance of NOE interactions. Under normal circumstances NOE

intensity may not be interpreted quantitatively for distance relationships. Typically three different mixing times are used and NOE are restrained to $2.7\text{\AA} < 3.5\text{\AA} < 4.5\text{\AA}$. Using this NOE information and the information obtained from NOEs may be used for distance constrained modeling of the peptide. This approach to NOE assignment and computer modeling is described in detail by Wuthrich¹⁵.

In order to obtain this information it is first necessary to obtain complete, or near complete proton assignments. To this end the 2-D TOCSY (Total Correlation Spectroscopy) experiments, also known as a HOHAHA, is a very useful tool. This experiment allows correlation of the aliphatic side chains to the amide protons of each residue²⁰.

When other information is lacking, either because of overlap or low sensitivity it is possible to gain some information from the chemical shift of an amino acid as determined by its magnetic environment²¹. However, such information is quite crude and should be interpreted very generously.

Despite the existence of several experimental probes for studying helix formation in peptides, it is also useful to be able to make some general predictions of the helical structure of peptides. Computer modeling is a powerful tool for this purpose. Because these small peptides have relatively simple structure as compared with proteins and because the basic structure of the peptides can be readily predicted, it is possible to obtain a visual picture of the interactions in the peptides through the use of some rudimentary modeling techniques²²⁻²⁴.

In this study computer modeling was achieved using MacroModel v3.0 on a VAX system. MacroModel is an integrated program for building and studying organic, bioorganic and biological molecules²⁴.

The modeling was performed by applying energy minimization functions based on the AMBER force field. This force field, designed explicitly for the study of proteins and nucleic acids involves a number of algorithms which have been found to accurately describe a broad range of interactions typically found in proteins²⁵. Energy minimizations are non-linear optimizations of the force field equation. In this method the computer calculates the energy of each atom based on its location; a new set of coordinates are then calculated in an effort to lower the overall energy of the molecule²⁴.

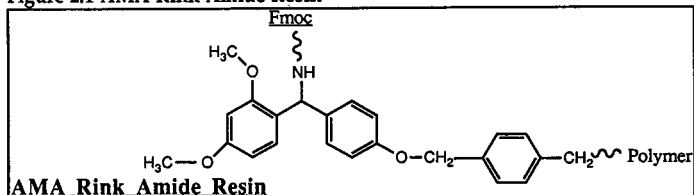
One of the major problems of computer modeling is the fact that the modeling algorithms will often become trapped in the shallow energy well of a local minima, and fail to find the global minima of the molecule. This can be particularly problematic if the molecule does not have one particularly stable structure and therefore has a very shallow global minima, or is lacking a large global minima altogether. One method of by which the influence of global minima may be avoided is the use of different starting geometries for the molecule. Therefore the models of various peptides were made in both the α -helical and the 3_{10} helix to provide different starting conformation from which to evaluate the modeling. A good general discussion of computer modeling its methods and limitation is available in reference 24.

Chapter 2
Experimental

MATERIALS

Four peptides were synthesized from a combination of four amino acids. The peptides were synthesized using a solid phase Fmoc synthesis as outlined in Jones¹³. Fmoc is 9-Fluorenylmethoxycarbonyl used to protect the nitrogen terminus of the amino acid during synthesis. Active side chains of the amino acids were blocked with t-butyl and Boc (t-Butoxycarbonyl) as appropriate. The amino acids were purchased from Novabiochem as the Fmoc and side chain protected derivatives of the amino acids. The amino acids used were N-epsilon-Boc-N-alpha-Fmoc-L-Lysine, N-Fmoc-L-Glutamic acid-Gamma-t-Butyl ester, N Fmoc-L-Alanine and N-Fmoc-o-t-butyl-L-Tyrosine. The solid phase support used is Rink Amide Resin 4-(2',4'-Dimethoxyphenyl-Fmoc-aminomethyl)-phenoxy resin. It is composed of Fmoc-Rink amide linker on polystyrene with 1% DVB cross-linking (Figure 2.1). The resin has a surface area for synthesis equivalent to 0.39mMol/g. The above reagents were obtained from Novabiochem. Acetic acid anhydride used in capping the peptide was purchased from Aldrich.

Figure 2.1 AMA Rink Amide Resin



Benzotriazol-1-ylxy-tris-(dimethylamino)-phosphonium-hexafluorophosphate (BOP) and N-Hydroxybenzotriazole (HOBT) are used as coupling agents during the synthesis. Both reagents are obtained from

Novabiochem. *N,N*-Diisopropylethylamine (DIEA) is used as a hindered base during coupling and is obtained from Aldrich.

N,N-Dimethylformamide (DMF) is used as the solvent for the synthesis. Trifluoroacetic acid (TFA), phenol, anisole and thioanisole are used during the cleavage of the peptide from the resin and cleavage of the side chain protecting groups. Piperidine is used during the deprotecting of the amino acid. These were also purchased from Aldrich.

SYNTHESIS

All syntheses were done with approximately 0.5g of resin. An attempt to use 1g of resin resulted in extreme difficulty for the addition of the first amino acid and was discontinued. The fresh resin was allowed to soak in DMF for 15min prior to beginning any synthesis in order to allow for complete solvation of the surface of the resin. A general outline of the Fmoc synthesis from Jones (13) is as follows. 1) Deprotection of the Fmoc, 2) washing of the resin and peptide, 3) addition of the amino acid, 4) washing of the peptide and 5) test for complete addition. The synthesis was carried out with the aid of a mechanical shaker. An outline of the synthesis procedure is given in Table 2.1. The reaction vessel size is approximately 100ml and is equipped with a sintered glass filter for vacuum filtration (Figure 2.2). All solvents and reagents are removed during the synthesis by vacuum filtration. The peptides are grown from the carboxyl terminus. The following peptide sequences were made.

KE5 Ac-YKAAE-NH₂

EK5 Ac-YEAAK-NH₂

EK3.3 and EK3.3a Ac-YEAAKAAEAAKAAEAAK-NH₂

EK4 Ac-YEAAAKAEAAKAEAAK-NH₂

Table 2.1 Protocol for Peptide Synthesis

(starting with 0.5g Fmoc-AMA-Resin 0.39mMol/g = 0.195mMol)

Wash I:

1. wash 100% DMF (15ml for 1 min. five times)
 - 1a. Kaiser test (peptide could be left over night at this step).

Deblock:

2. 30% Pip/DMF (15ml for 1 min, one time)
3. 30% Pip/DMF (15ml for 10 min, one time)

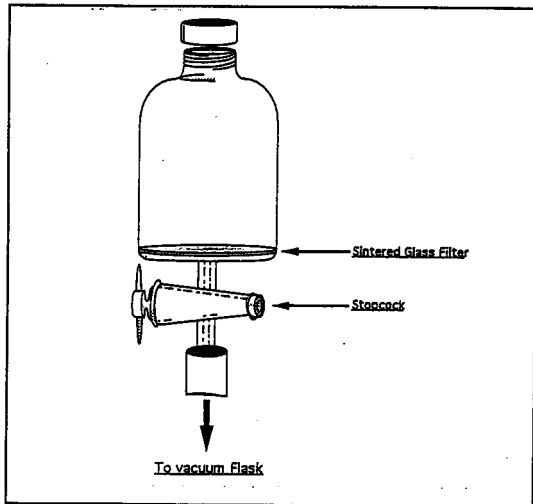
Wash II:

4. wash 100%DMF (15ml for 1min. 5 times)

Coupling: Fmoc-Amino Acid

5. 5eq. (0.975 g) of BOP (0.431 g), HOBt (0.132 g), Fmoc-Amino Acid weighed and put into flask
6. Add to bottle 5 mL DIEA/DMF, 0.195 mm/mL (5 eq of DIEA) and 5 mL of DMF.
7. Swirl & dissolve for 3 min.
8. Add solution to resin and let sit from 30-60min.
Repeat go to Wash I, step 1.

Figure 2.2 Reaction Flask



Deprotection

Both the resin and the amino acids are obtained as the Fmoc derivatives. The removal of the Fmoc is done using a 30% by volume solution of piperidine in DMF. Approximately 15ml of the deblocking solution was added to the reaction vessel containing the peptide and was allowed to react for approximately 1min and then removed by suction. It is assumed that approximately 90% of the Fmoc group is removed in this step. A second addition of 15ml of piperidine was added and allowed to react for 10min to remove any remaining Fmoc. The removal of the Fmoc is assumed to proceed as presented in Figure 2.3. After deprotection the peptide was washed 5 times with 15ml of DMF to remove any of the remaining deprotecting solution. Any remaining deprotecting solution could remove the Fmoc group of the amino acid during the next addition and cause multiple additions of the amino acid. The deprotecting solution should be made fresh at least every two to three days to avoid poor yield and multiple products.

Coupling

Five fold excess of the peptide and the coupling reagents, HOBt and BOP, were used. The coupling reagents were weighed into a 100ml coupling reaction vessel with a ground glass top. The reagents were shaken with 5ml of the coupling solution of DIEA and DMF with a one to one ratio DIEA to amino acid (0.195M DIEA), for 3min prior to addition to the reaction vessel containing the peptide resin. The chemistry of this reaction is presented Figure 2.4.

Figure 2.3 Fmoc cleavage

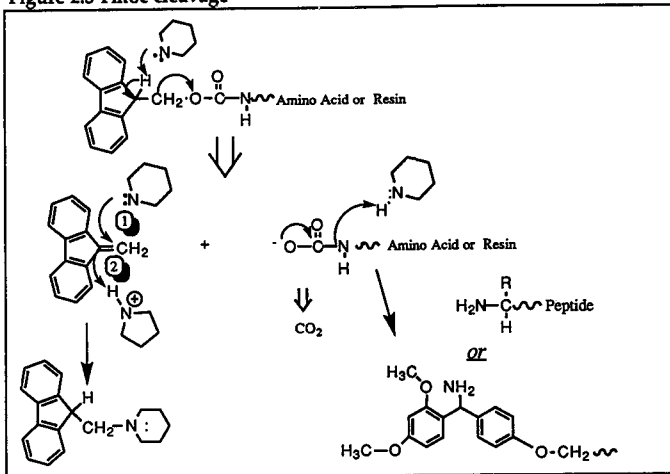
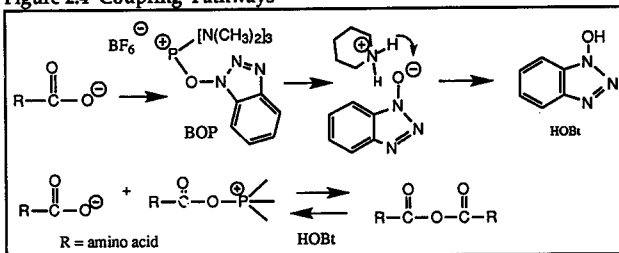


Figure 2.4 Coupling Pathways



DMF was used to rinse the coupling reaction vessel into the peptide reaction vessel. Enough DMF was added to provide an effective reaction volume of 15ml. The coupling solution contains 3.4 ml of DIEA and 96.6ml of DMF. The addition of the first peptide to the resin was allowed to react for one hour. Successive additions of amino acid were allowed to react for 30min to

one hour. The coupling of the amino acid is assumed to proceed as outlined in Figure 5. The coupling agents are removed and the peptide washed 5 times for one minute with 15ml DMF. At this point complete reaction of the exposed amides with the new amino acid is tested with the use of a Kaiser test²⁶. If the test was failed the coupling step was repeated. The deprotecting solution should be made fresh at least every two to three days to avoid poor yields and multiple products.

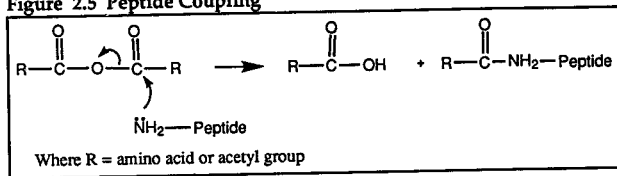
The Kaiser test was by preformed placing a small sample of the peptide and resin (typically a few beads) into a small test tube. To this was added two drops of 0.0002M KCN, (Prepared by dissolving 33mg KCN in 50ml of H₂O and diluting 2ml of this solution with 98ml pyridine.) , two drops of 0.28M ninhydrin in n-butanol and two drops of 80% wt/wt phenol/n-butanol. This mixture was then placed in a boiling water bath for 5min. A pale yellow or pink solution was taken to indicate 99.5% or better addition of the amino acid²⁶.

Capping

This is done similarly to the coupling. Five fold excess of the acetic acid anhydride and the 5ml of the DIEA/DMF coupling solution were added to a coupling reaction vessel and allowed to react for 3min prior to addition to the reaction vessel containing the peptide resin. DMF is used to rinse the coupling reaction vessel into the peptide reaction vessel. Enough DMF is added to provide an effective reaction volume of 15ml. The coupling of the acetyl cap is assumed to proceed as outlined in Figure 2.5. The DIEA, DMF and excess acetic acid anhydride is removed and the peptide resin is then washed 5 times for one minute with 15ml DMF. This reaction is also tested for completion using a Kaiser test. HOBt and BOP should not normally be added

during the capping, however, this was done for capping of the EK5, KE5, EK3.3 and EK4. This is thought to have had no effect.

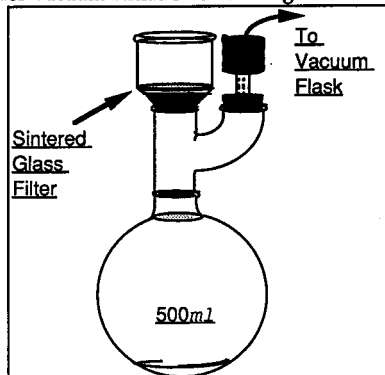
Figure 2.5 Peptide Coupling



Cleavage

The peptide resin is removed from the reaction flask manually and placed in a round 50mL bottom flask. The peptide resin and flask are then placed overnight in a vacuum desiccator pumped through a liquid nitrogen trap to remove any remaining solvent, acetic acid or water which might interfere with the cleavage. The next day the flask was set up for magnetic stirring and 15ml of the cleavage mixture was added to the flask containing the peptide resin and allowed to react for 2hr with constant stirring. For the KE5 peptide this cleavage mixture was 95% TFA and 5% phenol by weight. For all other peptides a mixture of 90% TFA and 5% anisole and 5% thioanisole by weight was used. This modification was made based on a cleavage mixture suggested by King et al²⁷ which gave very pure cleavage. The TFA solution and peptide was then filtered into a 500 mL round bottom flask using a sintered glass filter and vacuum filtration (Figure 2.6). The reaction flask and the resin were washed three times with cleavage mixture which is filtered into the 500mL flask for a total of 30mL of cleavage mixture and peptide.

Figure 2.6 Setup for Vacuum Filtration of Cleavage Mixture



This solution was placed on a rotovap equipped with a dry ice acetone trap for collecting the evaporated TFA. The solution was evaporated down to approximately 10mL. 100-120mL of cold anhydrous ether was then added drop wise to the flask. The mixture was allowed to precipitate overnight.

The next day the peptide precipitate was filtered from the ether using a sintered glass filter and vacuum filtration. The precipitate was washed three times with anhydrous ether and placed in a vacuum desiccator equipped with a liquid nitrogen trap.

The peptide is cleaved from the resin and the side chain protecting groups are cleaved from the peptide in this single step. Chemistry for this step is presumed to proceed as outlined in Figure 2.7 & 2.8.

Figure 2.7 TFA Side Chain Protecting Group Cleavage

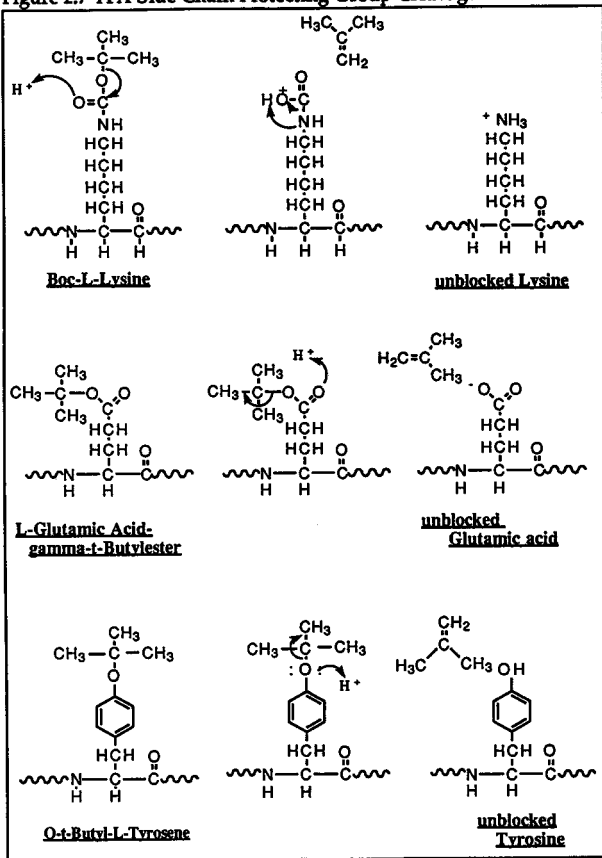
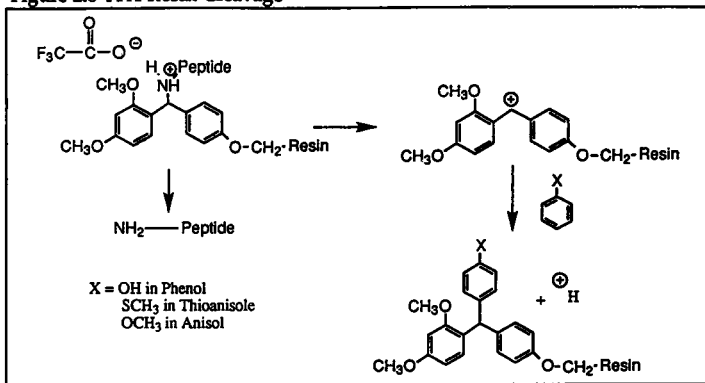


Figure 2.8 TFA Resin Cleavage



ANALYTICAL

HPLC

Analytical measurements of the purity of the crude peptide were made using a BSA HPLC. Chromatographs were taken at 95% water 5% acetonitrile nominal. The solvents each contained 0.1% TFA. The water also contained 1% acetonitrile. The column used is a C18 stationary phase with a 3micron packing, 100x3.2mm. The samples were dissolved in water with 1% acetic acid. Attenuation was set at 0.1-0.005. The concentration of the solutions used was:

KE5.	3.0mg/10mL
EK5	3.1mg/10mL
EK3.3	1.9mg/10mL

Absence of significant peaks in chromatograph of the of KE5 and KE5 is taken as good indication of reasonable purity.

HPLC preparatory work was also done for the EK5 peptide using a

200 μ l sample loop and exactly the same conditions as the analytical run. 75mg of peptide was dissolved in 2ml of water and 1% acetic acid. The samples were injected in 100 μ l units and the proper eluent collected. The excess solvent was evaporated by a rotovap equipped with a dry ice acetone bath. The peptide was transferred to a plastic sample vial using three 1mL washings of water. This sample was then lyophilized to remove the water.

UV-Absorption

UV spectra of the EK5 peptide in 1% acetic acid were taken at pH 3, 6, & 10. Spectra of tyrosine and phenol in water and 1% acetic acid were also acquired under slightly acidic conditions. The spectra were acquired using a HP8452A diode array spectrometer. Maximum from these measurements were used in the HPLC purification²⁸.

NMR

Spectra were acquired on a 200MHz Varian Gemini 200. 1-D proton spectra and 2-D spectra of the KE5, EK5 and EK3.3a peptide were acquired.

Concentration for the KE5 peptide was approximately 10mg/0.7mL of D₂O. No salt was added to the solution. Spectra were taken at pD2.9. 1-D experiments of the KE5 peptide were conducted with 16 transients. No resolution enhancements were used.

Concentration for the EK5 peptide were approximately 15-20mg/0.7mL of D₂O. To reduce the residual HOD peak many samples were completely prepared, lyophilized and redissolved in 99.9% D₂O (from sealed ampules) and the spectrum re-acquired. 1-D experiments of the EK5 peptide were conducted with 1024 transients and zero filled to 32K. Two dimensional

experiments were acquired with 128 or 256 increments in the t_1 dimension, with 128 to 256 transients. All 2-D spectra were zero filled to 1K by 1K. Resolution enhancement functions were applied to all spectra. Integration (Appendix 3) was performed on spectra to which no enhancements were applied. All samples were acquired while spinning the except the pD 7.0 DQF-COSY and one of two pD 11.3 DQF-COSYs.

Samples of the EK5 peptide were prepared at varied pH. This was done in order to determine pH dependent conformational changes and to aid in peak assignments. At pH 2.9 all residues are protonated. At pH 7.0 glutamic acid is deprotonated while lysine is protonated. This will encourage ionic interactions of the two oppositely charged side chains. At pH 11.3 lysine and tyrosine are deprotonated. Samples were prepared at 0.1M NaCl to provide a ion buffer for the pH studies. The EK5 peptide is slightly less soluble at pH 11.3 and a small amount of precipitate formed.

Samples of the 18-mer peptides were dissolved in 90/10% D₂O/H₂O at pH 5.5. Salt solutions are known to increase helicity, therefore, solutions were made at 0.1M NaCl. This will also act as a ion buffer for future studies. Peptide concentrations of 1-3mMol were used. The Experiments were conducted at New York University on a Varian Unity 500MHz instrument.

Mass Spectra

Mass spectrum of the EK3.3 and EK4 peptide were acquired at New York University using a quadrupole mass spectrometer with electrospray ionization.

Chapter 3

Results & Discussion

PEPTIDE SYNTHESIS AND PURIFICATION

The crude yield was satisfactory for the KE5, EK5 EK3.3a and EK4.0 peptides. Yield was generally between 85% and 95%. However, the EK3.3 peptide showed a poorer yield at approximately 55%. The weight of peptide collected after cleavage from the resin and the percent yield of the crude product is given in Table 3.1.

It is believed that the poor yield of the of the EK3.3 peptide was resulted from the long duration of the EK3.3 synthesis, which was performed over a period of approximately a week and a half, without making fresh reagents daily. During this period it is possible that the coupling and or deprotection reagents partially decomposed, resulting in poor reactivity and therefore poor yield. Alternatively, the EK3.3a peptide, synthesized over a three day period with new reagents made every day showed the highest yield of the 18-mer peptides.

Table 3.1 Weight and Yield of Peptide Synthesis

	Total Weight of peptide collected	Theoretical yield	Percent Yield crude product by weight
KE5	138mg	145mg	96%
EK5	137mg	145mg	95%
EK3.3	224mg	418mg	54%
EK3.3a	390mg	418mg	93%
EK4.0	360mg	418mg	87%

Purity of the synthesis of the 18-mers was checked at NYU by the use of the electrospray mass spectroscopy. The spectrum of the EK3.3 peptide showed very low purity. This large amount of impurity would be difficult to purify with the use of HPLC. For this reason the EK3.3 peptide was re-

synthesized. This new EK3.3 peptide was designated EK3.3a. Qualitative interpretation of the spectra of the EK3.3a and EK4.0 peptide showed purity on the order of 80%. On the basis of this information the EK3.3a peptides and EK4.0 peptides were assumed to be of sufficient purity of assignment of chemical shift and preliminary studies of conformation. For further discussion of the purity of the peptides see the thesis by Jay Berger²⁸.

1-D proton NMR spectra of the 5-mer peptides showed few peaks which could not be assigned to the peptide. On this basis, purity of the peptide was assumed to be sufficient for further NMR studies.

COMPUTER MODELING

Computer modeling studies of the EK3.3 and EK4.0 peptide were carried out. This was done to give some insight into some of the interactions which may be taking place in the peptides. In particular, does the computer modeling predict the salt bridge interactions which we are attempting to create in the EK3.3 peptide? The modeling also provides a reasonably accurate picture of the peptide from which to hypothesize about additional interactions in the peptide.

The exact parameters for modeling of the peptides is given in Appendix 1.1-2. This appendix shows an example of the .com files which were submitted for minimization and a copy of part of the MacroModel output file. The parameters input were essentially those recommended in the MacroModel BatchMin v3.1 manual. A solvent parameter was included in the modeling to more accurately simulate the structure of the peptide in water. MacroModel solvent model 3 was used, This model includes a parameter for solvent accessibility and a term for electrostatic polarization.

This model is recommended in the MacroModel manual. For a detailed explanation of the parameters input in the .com file refer to the MacroModel manual. Starting conformations for the modeling were approximately α -helical. Modeling with 3_{10} helix starting conformations was also attempted but have not been completed at this time.

In our modeling glutamic acid was deprotonated and lysine protonated so as to simulate neutral pH conditions which would promote of salt bridging formation.

The lowest energy model of the EK3.3 peptide shows close association and hydrogen bond formation between glu2 & lys5, glu8 & lys12 and glu15 and lys18 in the $i,i+3$, $i,i+4$, $i,i+3$ salt bridge pattern. Other higher energy models showed hydrogen bond formation between different combinations of neighboring lysine and glutamic acid. One model also showed interaction between glu2 and tyrosine. Examples of the lowest energy model of the EK3.3 peptide are shown in Appendix 1.2.1-2. The orientation of the tyrosine away from the helix in this model is believed to be a function of the modeling starting conformation and may not be representative of the actual conformation of tyrosine. All models of the EK3.3 peptide showed significant helical content.

Our model of the EK4.0 peptide showed the $i,i+4$ salt bridging predicted. The association between the ion pairs is not as close as the association seen in the EK3.3 peptide but this may be due to the lesser number of iterations performed on the EK4.0. This association would therefore be expected to improve if further iterations were carried out. Two views of the EK4.0 model are available in Appendix 1.3.1-2.

It is interesting that the lowest energy conformation of the EK3.3 peptide shows the formation of a hydrophobic face. The EK4.0 model the three salt bridged sections are evenly spaced about the face of the peptide helix, as predicted by Baldwin⁷. If this is an accurate structure this may explain some of the solution properties of the EK3.3 peptide in relation to the EK4.0 peptide. It is postulated that the even spacing of the salt bridging about the face of the EK4.0 peptide allows the formation of a hydrophobic groove and a hydrophilic ridge. Binding of two hydrophobic grooves, stabilized by interaction between oppositely charged side chains of two peptide chains, may form a double helix. This binding may be stronger than the hydrophobic face on face binding of the EK3.3 peptide, which cannot form the appropriate relationships for the interaction of oppositely charged side chains. This may explain why the EK4.0 peptide will only go into solution at concentrations below ~3mM while the EK3.3 peptide is soluble at concentrations above 20mM. This conclusion is supported by the NOESY spectra, which suggest that the EK4.0 peptide may be an aggregate forming a larger complex with a slower rotational correlation time¹⁵. The EK3.3a NOESY spectra shows no unusual effects. This effect may not have been noted in Baldwin's work as the concentrations of the solution may not have been sufficient for aggregation. Alternatively, this aggregation may be solely a function of our EK4.0 peptide which includes an extra alanine between lysine and glutamic acid as compared with the Baldwin EK4 peptide (e.g., KAE vs. KE). This alanine would serve to increase the size of the hydrophobic groove of the EK4.0 peptide. A suitable model of comparison, in our case the EK3.3 peptide, may also have been lacking.

Both the EK3.3 and EK4.0 model showed significant helicity in the models. Given that the starting conformations were α -helical and that alanine itself has strong helical tendencies, this is not surprising.

NMR STUDY OF THE 5-MER PEPTIDES

Mathematical Resolution and Sensitivity Enhancement

Small peptides are relatively complicated molecules to study by NMR. The investigations performed here are even more limited in that the instrument setup is not optimal for peptide studies. In order to make optimal use of the instrument available, several resolution enhancing functions were applied directly to the NMR FID.

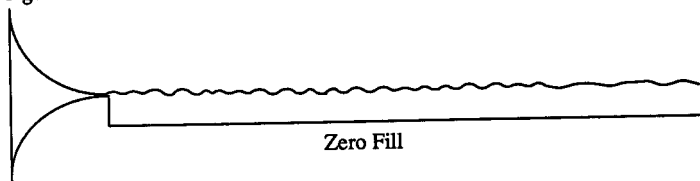
The early part of a FID contains coarse information on the peak frequencies. The later part of the FID contains fine information on frequency differences, e.g., whether there is one peak at 200 Hz or two peaks at 199 Hz and 201 Hz. The longer the FID signal is detected the greater the resolution of the spectrum. This is why the acquisition time is such an important parameter in detection. Applying functions which emphasize the tail of the FID improves resolution. Applying functions which emphasize the beginning of the FID improves sensitivity.

Resolution and Sensitivity Enhancing Functions

A "zero fill" function takes advantage of the fact that the NMR FID is sinusoidal and quickly decays. Interpolating zeros at the end of the FID function improves the resolution of poorly digitized peaks (Figure 3.1.). The zero fill function is considered to be primarily cosmetic but is useful in resolving poorly digitized peaks. Thus, by application of this function it is

possible to take advantage of the fact that computer time is cheap while spectrometer time often is not. This also avoids the acquisition of noise which does not improve the spectrum. This function has little effect on peak intensities so integration after zero fill is still possible. In our experiments using the Varian Gemini 200 this function was applied by setting FN=32000 for 1-D and FN and FN2=1024 for the 2-D experiments where increments in the 2-D are typically NI=512 and NI2=128. An example of the application of this function to a spectra is shown in Appendix 2.1, 2.2.

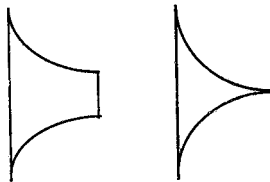
Figure 3.1 FID Zero Fill



A line narrowing function provided the largest component of sensitivity enhancement. Applied to the tail of the FID this is an exponential increasing function which results in a narrowing of lines in the transformed spectrum. However, this function also induces truncation wiggles which must be suppressed by the use of a window function. Moreover the function affects peak intensity unevenly so integration is not possible. As this function degrades signal-to-noise ratios, spectra to which it is applied must have high signal to noise ratios. In our experiments this function was applied by the command RE. RE=0.300 was found to give good resolution with acceptable amounts of distortion. This function was applied only to 1-D experiments.

Fourier transformation cannot accurately convert sharp transitions, as such transitions cannot be built up from a combination of sine waves. The nearest approximation of a sharp transition incorporates a decaying sine wave at the end of the peak in the transformed spectrum. These sine waves are called truncation wiggles. Window functions or apodisation functions convert sharp transitions in the FID into more gentle transitions which may be accurately Fourier transformed. The application of this kind of function is especially important in 2-D experiments with short acquisition times. An illustration of the application of this kind of function to data acquired with a short acquisition time is shown in Figure 3.2. In our experiments this function was applied with the command AF and AF2. $AF=0.598$ was found to give a reasonable 1-D spectrum.

Figure 3.2 Application of a Window Function



The particular type of window function applied was a Lorentzian-Gaussian transformation. This function also emphasizes the end of the FID. As a result, the peaks in the transformed spectra are converted from broad tailed, Lorentzian type peaks, to narrow tailed, Gaussian type peaks. The function can also have line narrowing effects. Thus, resolution enhancement is achieved by a combination of zero fill, line narrowing and apodisation functions. By emphasizing the tail end of the spectrum the Lorentzian-Gaussian transformation causes a suppression of peaks and a significant

reduction in signal-to-noise. An example of the improvements achieved by application of all three functions to a spectrum from our experiments is shown in Appendix 2.3.

All three functions (RE, AF, FN) may be applied automatically with the RESOLV command. However, the line narrowing function (RE) applied is a bit severe. Alternative functions were not fully explored in the time available. One function reported to be particularly useful in 2-D experiments is the sine-bell function. This function was not available on our instrument. A discussion of many of these functions is available in several NMR texts^{15,29,30,31}. Zero fill and window functions were applied to all 2-D spectra. A sensitivity enhancing function, automatically applied to all of our 2D experiments, is essentially the opposite of the line narrowing function. This function may be controlled by SE, SE2, LB, and LB2. The exact mathematical equations of the functions applied by the software can be found the Gemini operation manual.

All 2-D experiments were symmetrized about the diagonal. This takes advantage of the fact that the spectrum should be symmetrical as the two axes are symmetrical. Noise on the other hand is not symmetrical and will be removed. This function is applied by typing FOLDT after Fourier transform.

Shimming

To obtain the best resolution and sensitivity from the instrument it is important the instrument be well shimmed, preferably, at least one HIREs shim should be run before performing any experiments on a new sample. Most 1-D experiments were acquired with 1024 transients in order to improve signal-to-noise which is degraded by the resolution enhancing functions.

Temperature

All experiments were run at 25.0°C to provide a constant temperature at which to compare spectra and to avoid peak broadening by temperature drift during acquisition. Temperature may be controlled by typing TEMP=25.0 and SU. The sample must be allowed to equilibrate before acquisition. Shimming must be performed at the temperature at which the experiment is to be performed.

Spinning

In some situations the two dimensional experiments appear to provide a simpler spectrum with better line shape when the sample is not spun. This may be due to the reduction of artifacts such as spinning side bands and t_1 noise. In the 1-D spectrum not spinning the sample reduces resolution because of increased inhomogeneity. However in the 2-D experiment the digital resolution is insufficient to distinguish such detail and the reduction of artifacts becomes paramount.

A spectrum of the EK5 taken on the NYU Unity 500MHz provides an interesting comparison to a 200MHz spectrum and is shown in Appendix 3.7.

Assignments of chemical shift

In evaluating the chemical structure by NMR the first step is the assignment of chemical shifts which are distinctive for individual nuclei. Once overlap in peaks is resolved, it is usually possible to assign unique chemical shifts for most nuclei in the structure. In the case of peptides one common strategy is to assign amino acid side chain protons in D₂O before moving to water solution and assignments of exchangeable protons. This

method of assignment was chosen in our investigation of the EK5 and KE5 peptides in order to overcome some of the instrumental limitations and to avoid the complications of solvent suppression when attempting unfamiliar experiments.

We found that the 1-D proton NMR studies showed relatively good resolution of individual peaks for the EK5 and KE5 peptide. The differences between the two spectra at pD 2.9 were almost insignificant. A COSY spectrum of the KE5 was taken for comparison to the EK5. However, relatively little analysis was done of the KE5. The assignments for the KE5 as determined from the 1-D and the simple COSY are given in Table 3.2.

Table 3.2 Proton Assignments of the KE5 peptide in ppm

	a	b	g	d	e	aromatic
Y	4.36	2.9	---	---	---	6.74, 7.03
K	4.1	1.6	1.25	1.5	2.8	---
A	4.2	1.31	---	---	---	---
A	4.2	1.31	---	---	---	---
E	4.25	1.95	2.38	---	---	---
Ac	1.95	---	---	---	---	---

We undertook a more detailed analysis of the EK5 peptide. Spectra were taken at pD 2.9, 7.0 and 11.3. At pD 7.0 a significant shift was seen in the triplet from 2.31ppm at pD 2.9, to 2.16ppm at pD 7.0. It is believed that this corresponds to a deprotonation of glutamic acid which shifts the gamma hydrogens up field. In all three spectra the aromatic peaks were clearly visible.

It was obvious that a complete assignment of the EK5 peptide would not be possible from our 1-D experiments. Fortunately a large number of 2D

experiments have been developed since 1972 to allow a much more complete evaluation of the EK5 peptide.

TWO DIMENSIONAL EXPERIMENTS

J-Resolved

Historically, the first 2-D experiment was the J-resolved experiment²⁹. With this method the first dimension is the chemical shift with coupling pulled in to the second dimension. This experiment is very fast for a 2D experiment, resulting from the small number of increments in the second dimension. Although, it is highly sensitive, it provides only a limited improvement in resolution over one dimensional experiments. Thus it has been almost entirely supplanted by other experiments. Our J-resolved spectrum of the EK5 peptide is show in Appendix 3.6.

COSY

The most useful experiments in our assignment of the EK5 peptide was the COSY (COrelation Spectroscopy) and its variations. The pulse sequence for the COSY experiment is provided in Figure 3.3. A simple explanation of the COSY experiment follows. Nuclei are excited with a 90° pulse. A given nucleus is allowed to correlate with another nuclei during the time increment t_1 . A second 90° pulse is applied to move the magnetization of non-correlated nuclei from the xy plane, into the -z plane, rendering it unobservable. The COSY experiment is the most sensitive of the two-dimensional experiments performed, with the possible exception of J-resolved. This sensitivity, in part makes it one of the fastest 2-D experiments^{29,31}.

The simple COSY, however, has some serious limitations. One problem is that very little splitting is seen in the COSY spectrum due to the low resolution of 2-D experiments. In order to limit acquisition time of two-dimensional experiments it is common to use only a small number of increments in the second dimension. In our experiments the second dimension included 128 increments. This gave only 9Hz resolution in second dimension (spectral width = 6ppm = 1200Hz, $1200\text{Hz}/128=9.34\text{Hz}$). In the first dimension with 512 increments, resolution was slightly better at approximately 3Hz. This compared with a digital resolution in the one dimensional spectrum of 0.1Hz or better.

A second problem with the COSY experiment is that the diagonal peaks tend to be fairly strong. The diagonal peaks arise from the movement of longitudinal magnetization (magnetization on the z axis) to the xy plane with the application of the second 90° pulse. This magnetization is not correlated with that of another peak and so gives rise to the diagonal. This strong diagonal may obscure close peaks. Lysine gamma-delta peaks very often do fall very close to the diagonal (gamma shift $\sim 1.7\text{ppm}$ delta shift $\sim 1.4\text{ppm}$). In fact there does appear to be a cross peak in this region in the spectrum of the EK5 peptide. Nevertheless, such an assignment would be tentative based solely on the COSY data. It is generally concluded that the problem of cross peaks overlapped with the diagonal will not be completely addressed by a simple improvement in resolution.

It was possible to make a large number of assignments in the EK5 peptide. However, several unresolved peaks demonstrated that an improved experiment was desirable.

DQF-COSY

Fortunately an experiment exists which addresses both the problem of low resolution and strong diagonal in the COSY experiment. This experiment, the Double Quantum Filtered COSY (DQF-COSY)^{17,29,30} includes two methodological improvements from a simple COSY. The pulse sequence for this experiment is given in Figure 3.3.

First, the DQF-COSY is a phased experiment. The NMR signal contains both a real and imaginary component. By phasing the experiment to show both positive and negative peaks it is possible to display both real and imaginary peaks simultaneously. The practical result is that the fine splitting in multiplets may be resolved by phasing peaks oppositely to each other. Thus the effective resolution is increased without a real increase in the digital resolution.

In the Varian Gemini 200 the phased spectrum is generated using the States method²⁹. In this technique two spectra are acquired for each t_1 increment. The first spectrum serves as the real data. In the second spectrum a phase change is brought about by shifting the phase of both the first pulse and the receiver or alternatively by shifting the phase of the second pulse by -90° . This second spectrum generates the imaginary (or anti-phase) component of the spectrum²⁹. Since two separate spectra are acquired, phased experiments take twice as long as non-phased experiments.

We found that when displaying phased experiments it is important that the experiment be phased correctly. To achieve proper phasing with the Gemini 200, after acquisition of the spectrum, type:

WFT(2), this will Fourier transform a 1-D slice of the second spectrum. Phase this spectrum for pure absorption and Fourier transform the entire spectrum with the WFT2DA command.

The second change in the DQF-COSY from the simple COSY is the use of a double quantum filter. Single quantum coherence is the only observable type thus, double quantum coherence must be converted into single quantum coherence to be observed. In order to do this a third pulse is applied almost immediately after the second pulse of a COSY pulse sequence (delays of a few μ s between the second and third pulse are typical). This pulse converts most of the double quantum coherence which has been evolving along with the single quantum coherence, into observable single quantum coherence. This newly generated single quantum coherence is distinguishable from the existing single quantum coherence because p-quantum coherence is p-times more sensitive to phase shifts than single quantum coherence. In other words, double quantum coherence is twice as sensitive to phase as single quantum coherence. The phase change may be detected by shifting the phase of the first two pulses by 90° relative to the third pulse, this results in inversion of the signal detected via double quantum coherence. Shifting the phase of the receiver by 90° then selects for the component derived from double quantum coherence^{17,30,29} (These sections on phased experiments and double quantum filters were paraphrased from Derome chapter eight²⁹.)

The diagonal peaks and many solvent peaks are suppressed in the double quantum spectrum. These peaks which result from resonance of single protons, which cannot evolve double quantum coherence. The amount of suppression of single quantum coherence varies, being dependent on several factors including the t_1 increment and coupling²⁹. Suppression of single quantum coherence is limited, but may be as large as a several

hundreds times the original intensity. Although substantial, this method of solvent suppression alone is not sufficient for observation of spectra in water^{15,29}. Theoretically the use of a double quantum filter should show a two times reduction in sensitivity, however, in practice this use of a double quantum filter is often not the limiting factor in sensitivity of 2-D experiments. The difference in sensitivity between the DQF-COSY and a simple COSY can be quite small.

The DQF-COSY is implemented on the Gemini 200 by typing DQCOSY while in experiment 4.

Relayed COSY

In our DQF-COSY of the EK5 peptides the cross-peak at 1.4ppm and 1.7ppm were more clearly resolved than in the simple COSY. However, it still might be argued that this are an artifact of the diagonal. Additionally, the EK5, lysine alpha- beta cross peak is not resolved in any of the different, pD, DQF-COSY spectra. In an attempt to resolve some of these problems a relayed COSY was performed. This experiment allows correlation of longer range coupling than is typically seen in the COSY experiments. The relayed-COSY may resolve overlapped peaks, by duplicating proton resonances in overlapped spectral regions, in a less complicated spectral region. The pulse sequence for relayed COSY we used can be found in Figure 3.3.

The explanation of this experiment is analogous to the COSY. The third 90° pulse develops correlation to a third proton, and the 180° degree pulse removes the chemical shift of the third hydrogen, aligning it with the normal COSY cross peak. Correlation with the a third hydrogen is determined by the delay time τ , which is varied for different couplings

and spin systems. This experiment gives good correlation of peaks with strong coupling but may lack correlation for weak coupling, as the signal may decay before adequate coherence develops. We used a fixed delay of 35ms for τ , which gives good correlation for a 7Hz coupling in several different types of spin systems³². As expected we found that long range correlations developed in this way were weaker than the normal COSY cross peaks.

This experiment may be implemented by typing RELAYH in experiment 4. (Note: the Gemini variable tau is $1/2\tau$)

Our relayed COSY of the EK5 peptide at pH 7.0 showed one new cross peak at 2.95,1.4ppm (Appendix 3.10). The presence of this peak proved useful in identifying the lysine spin system. The peak assignments as they could be determined for the EK5 peptide from these experiments are presented in Table 3.3.1-3. (Note: The assignments given for alanine are not meant to imply the sequential assignment)

Table 3.3.1 EK5 pD 2.9 Proton Assignments in ppm

	α	β	γ	δ	ϵ	aromatic
Y	4.42	2.9	---	---	---	6.79, 7.08
E	4.25	1.8	2.35	---	---	---
A	4.2	1.35	---	---	---	---
A	4.2	1.36	---	---	---	---
K	?	?	1.4	1.65	2.31	---
Ac	1.95	---	---	---	---	---

Table 3.3.2 EK5 pD 7.0 Proton Assignments in ppm

	α	β	γ	δ	ϵ	aromatic
Y	4.44	2.95	---	---	---	6.79, 7.09
E	4.1	1.8	2.2	---	---	---
A	4.15	1.36	---	---	---	---
A	4.15	1.36	---	---	---	---
K	?	?	1.35	1.6	2.17	---
Ac	1.95	---	---	---	---	---

Table 3.3.3 EK5 pD 11.3 Proton Assignments in ppm

	α	β	γ	δ	ϵ	aromatic
Y	4.45	2.93	—	—	—	6.80, 7.05
E	4.35	1.80	2.17	—	—	—
A	1.35	1.37	—	—	—	—
A	1.35	1.40	—	—	—	—
K	?	?	1.75	1.65	2.95	—
Ac	1.94	—	—	—	—	—

Assignment of Coupling and Torsion Angles

Multiplets in DQF-COSY spectra are a complex problem requiring a somewhat detailed explanation. In the simplest case of the 1-D spectrum, the $n+1$ rule applies, where n is the number of hydrogens on atoms adjoining the protons of interest. In our spectra of the EK5 peptide this kind of coupling is seen in the alanine methyl peaks. However, the 1-D spectrum also shows a more complicated coupling pattern. We observe complex multiplets in the 1-D spectrum of the EK5 peptide, at 1.6ppm and 1.7ppm at pD 7.0. It is known from the 2-D spectrum that these two peaks correspond to the beta hydrogens of lysine and glutamic acid. According to simple coupling rules these two peaks should be quartets, however, a complex multiplet is seen for both of these peaks. The existence of a chiral center at the α carbon makes the beta hydrogens diastereotopic. Each beta hydrogen is now different and each hydrogen couples to the alpha hydrogen individually. Thus the alpha hydrogen splits into a doublet of doublets. In the 1-D spectrum such splitting would be obscured by the large amount of overlap among the alpha hydrogens. Observing these couplings in the beta hydrogens is more complicated because these beta hydrogens are coupled both to the alpha hydrogens, each other and the gamma hydrogens. This beta hydrogen to beta hydrogen coupling is typically on the order of 11.5Hz. In a 2-D experiment

coupling which occurs between nuclei not being directly observed (e.g., beta to beta hydrogen coupling) is known as passive coupling. The couplings of each beta hydrogen to the alpha hydrogen are of different strengths. This coupling is described by the empirically determined Karplus equation:

$$^3J_{H\alpha H\beta} = 9.5 \cos^2 \chi^1 - 1.3 \cos \chi^1 + 1.6.$$

This means that coupling between the two beta hydrogens and the alpha hydrogen can occur in several different combinations.

The combination of two small couplings between two beta hydrogens to the alpha hydrogen can be troubling. The lower limit for observation of coupling in the 1-D proton spectrum is typically 1 Hz²⁹ although the lower limit of observation of coupling in the Varian Gemini 200 is not known. The complex combination of coupling can be particularly problematic in the assignment of coupling of alpha-beta hydrogens in the phased DQF-COSY. The χ^1 coupling is restricted to two combinations, one large coupling (<4.0 Hz) and one small coupling (>3.0 Hz), or two small couplings (>3.0 Hz). In the situation where both beta to alpha couplings are small, overlap of oppositely phased peaks is more likely to occur in the 2-D multiplet, resulting in partial cancellation of peaks. This results in decreased intensity of the multiplet. This combination of splitting and partial cancelling out of peaks explains the reduced intensity of the glutamic acid alpha-beta cross peaks. This also provides one explanation as to why the lysine beta-alpha cross peak is not visible. Careful analysis of the phase of the peaks in the DQF-COSY allows resolution of the passive and active coupling. Peaks arising from active coupling will be of opposite phase while peaks due to passive coupling will be of the same phase. A good discussion of this effect can be found in Derome²⁹ p. 219. However, our data do not appear to be adequate for such an

analysis. In the future it may be possible to resolve the coupling of complex multiplets in the 200MHz spectra through use of primitive exclusion COSY experiments (P.E.COSY). This pulse sequence is available on the Gemini 200.

In determining torsion angles based on $^3J_{\text{H}\alpha\text{H}\beta}$ it is common to assign the beta hydrogens to one of three rotomers³³, -60° , 60° or 180° . It is possible to stereo specifically assign beta protons from the Karplus equation in the situation where there is one strong alpha beta coupling. When including these torsion angle constraints in computer modeling, these angles are typically restricted³³ to $\pm 60^\circ$.

Reduction of Peak Intensities

Another effect which may result in a reduction of peak intensity is a change in conformation, occurring slowly relative to the NMR time scale. In small molecules any conformation changes which are occurring are normally very fast relative to the NMR time scale. So the signals resulting from different conformations, which might place the protons in different magnetic environment are averaged into a single peak. Moderately fast conformational change can result in broadening of peaks and some degree of lessened sensitivity. However, it may be possible for a larger molecule to have two, or more, relatively stable conformations. In this situation the molecule may be undergoing slow transformation between these two states. This results in two totally separate peaks. In the case of the EK5 peptide, change in conformation would have little effect on the amino acid side chain resonances, as they are solvent exposed. Thus their chemical environment would change little in different conformations. However, alpha hydrogen chemical shifts of small peptides shows a strong correlation with

conformation. Therefore, these hydrogens would be more likely to be affected by conformational change. There is arguable evidence for the adoption of different conformations by the EK5 peptide. A new multiplet in the pD 11.3 DQF-COSY at 1.9,4.2ppm could be attributable to a second conformation of the deprotonated tyrosine. This new peak has essentially the same beta frequency of the other tyrosine peak but a different alpha resonance. Multiple conformations of tyrosine would be reasonable, as the 1-D spectrum shows minor peaks to either side of the tyrosine aromatic peaks. However, this cannot be taken as conclusive evidence for the existence of multiple conformation of the peptide, as no corresponding shifts are seen for the other residues. Other transformations may also be occurring too quickly to be observed. Alternatively, conformational change may be occurring slowly but simply be unresolvable due to decreased sensitivity for any of the reasons discussed. This may provide an explanation for the unobservable lysine alpha-beta cross peaks.

It is also possible to observe coupling between alpha protons and amide protons. However, in order to see amide protons the sample must be in a water solution. Under such conditions it is possible to see couplings between amide protons and beta protons. This coupling typically ranges from 2-11 Hz and is described by the empirically determined Karplus equation $^3J_{\text{NH}\alpha} = 6.4\cos^2\Theta - 1.4\cos\Theta + 1.9$ where $\Theta = |\phi - 60|$ (this relation of Θ to ϕ is often not mentioned in the literature)¹⁵. For α -helix structures, $\phi = -57^\circ$ (on average), which is equal to 3.9Hz coupling and for 3_{10} structures, $\phi = -60^\circ$ (on average), which is equal to 4.2Hz coupling. These couplings are very similar and while it is theoretically possible to measure such differences, to interpret

this as a difference between α and 3_{10} helix is not possible. However, it should be possible to use a series of such couplings as proof of helical content.

Water Suppression

In order to observe amide protons it is necessary for the sample to be in primarily a water solution. Solutions are typically made 90/10% water/D₂O with D₂O being present for the deuterium lock, although 50/50 solutions are sometimes used. However, the very intense water signal will overload the analog to digital converter as well as obscuring any peaks near it. In order to observe the spectrum of the peptide in water it is necessary to suppress the water resonance in some way. One method, common in peptide studies, is the use of a presaturation pulse--a presaturation pulse is a strong pulse applied directly to the water resonance prior to acquisition. It is possible to use this method in proteins and peptides where the conformation is reasonably stable and amide proton exchange occurs slowly. In the case of the EK5 peptides the amide protons may be exchanging somewhat more quickly than is typical in a peptide with a truly ridged structure. This exchange would cause weak amide proton resonance.

In our experiments water suppression was attempted on a 90/10% water/ D₂O solution of the EK5 peptide at pH 5.5. This is a pH where amide proton exchange is relatively slow. The best results were obtained with a decoupler offset of -95, pulse duration of 2sec, high power decoupler levels of 40-50 with the homonuclear decoupler on. Good spectrum were not obtained. This avenue research has not been fully explored in this project.

The Nuclear Overhauser Effect

The Nuclear Overhauser Effect (NOE) arises from direct dipole-dipole coupling of nuclei. The effect is analogous to the enhancement of the magnetic fields of two bar magnets placed close to one another¹⁸. In protons, the NOEs may arise from nuclei within 5Å of each other. In NMR, NOEs cause the enhancement of the longitudinal component of magnetization (magnetization on the z axis), a component often neglected in regular spectroscopy. The pulse sequence for measurement of NOEs in a two-dimensional experiment, is called a NOESY (Nuclear Overhauser Effect Spectroscopy) and its pulse sequence is shown in Figure 3.3. The first two 90° pulses generate coherence between nuclei as would be observed in the COSY experiment. However, a second delay, the mixing time (t_m), allows the evolution of NOEs between the two correlated nuclei. The third pulse applied, returns the NOE from the z-axis where it was generated to the xy-axis where its decay may be detected. This pulse also removes previously generated magnetization in the xy-axis. As might be expected this kind of experiment has very low sensitivity.

NOEs arise in through space dipole-dipole couplings. This makes them useful in determining the spacial conformation of peptides. However NOEs are dependent on a large number of effects. NOEs are proportional to $\omega_0\tau_r$ where ω_0 is Larmor frequency and τ_r is the rotational correlation time of the molecule. Thus both positive and negative NOEs may be obtained, depending on the rotational correlation time of the molecule. In the unfortunate situation where $\omega_0\tau_r$ equals approximately 1 no NOE will arise. NOEs may also be modulated by high frequency transitions with the

molecule itself. For instance if a peptide is shifting between two stable states and is in each conformation 50% of the time the NOE in each conformation will be 50% of what would be expected for a single conformation. If the conversion is relatively fast, on the order of τ_r then this factor too modulates the NOE. The combination of factors affecting the evolution of NOEs may be modulated by varying the mixing time. Different mixing times will provide more efficient NOE transfer for certain τ_r and for nuclei which are of different spatial relationships^{15,18}. NOE distances determined in this way are known as build up NOEs. The use of build up NOEs for spatial constraints in computer modeling of peptides is discussed by Wuthrich¹⁵.

Our NOESY of the EK5 peptide at pH 2.9 is shown in Appendix 3.12. This experiment failed to show significant NOE peaks for the EK5 peptide and little structural information was gained. A partial explanation may be that the EK5 peptide is likely to have a number of stable conformations. Moreover the Gemini instrument is inadequately setup for experiments such as NOESY which require high sensitivity. In particular the probe has been designed to maximize detection of broadband nuclei. This design means that the proton coil is outside the broadband coil—a factor that causes both a reduction in sensitivity and the introduction of artifacts in certain experiments. In contrast, probes designed to optimize proton detection may show a four fold or greater increase in sensitivity.

NMR STUDY OF THE 18-MER PEPTIDES

Our NMR study of the 18-mer peptides were carried out on a Varian 500MHz Unity instrument at NYU. The instrument was configured for direct proton detection. Samples were made at 1-3mM concentrations at pH 5.5

with 0.1M NaCl. At pH 5.5 amide proton exchange is slow and glutamic acid and lysine are available for salt bridge formation. The evaluation of the data from these studies is currently underway.

TOCSY

A TOCSY experiment was run to facilitate the assignment of the proton chemical shift. Using this experiment it is possible to show correlation of residue side chains to amide protons. This correlation is very useful for several reasons. First, the chemical shifts of amide protons occur over a very broad range, typically from 7-9ppm. Therefore, these protons are less likely to be overlapped than alpha or beta protons. Second, all amino acids have amide protons. Making correlation of aliphatic side chains with amide protons a convenient method of assigning chemical shift. (Obviously such experiments must be carried out in water in order to observe amide protons.)

The pulse sequence for a TOCSY experiment²⁰ is given in Figure 3.3. The experiment works by applying a 90° pulse and allowing correlation to other nuclei during t_1 , as in a COSY experiment. A spin lock pulse (a strong broad pulse applied in the xy-plane) is then applied to lock the transverse magnetization in the xy-plane allowing a polarization transfer of magnetization through chemical bonds. The efficiency of this transfer is modulated by several factors including distance and torsion angles. The experiment offers relatively good sensitivity and in general detect all protons for a given side chain.

In our experiment the EK3.3a peptide shows distinct resonances for 12 of the 18 residues (Appendix 4.5). In contrast the EK4.0 peptide showed

considerably more overlap, giving distinct resonances for perhaps eight residues (Appendix 4.3).

NOESY

We conducted a NOESY experiment on both the EK4.0 and the EK3.3a. The EK3.3a peptide provides a good NOESY spectrum with a 200ms mixing time (Appendix 4.6). For comparison the EK4.0 peptide, with the same mixing time, gives very poor spectrum (Appendix 4.4). It is speculated that the latter result was caused by aggregation of the EK4.0 peptide which produced an increase in its rotational correlation time. The relationship between molecule size and rotational correlation time is well established^{15,18}. Analysis of the decay time for the EK4.0 peptide may confirm whether this is the case. Improved results may be obtained with a different mixing time. However, given the quite severe overlap in the TOCSY spectrum the NOESY spectrum may be of limited use. Thus such a study was not pursued.

DQF-COSY

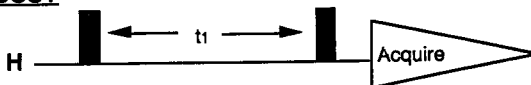
We acquired a DQF-COSY on the Gemini 200 of the EK3.3a peptide (Appendix 4.7.1-2). The spectrum showed good resolution and sensitivity. The peak shapes appear better than those of the EK5 peptide. This may be due to EK3.3a having a few closely related stable conformations, while EK5 may have several different conformations which could contribute to peak broadening. All four types of amino acid in the EK3.3a are resolved in the 200 MHz spectrum. However, the differences between amino acid of the same type were not resolved. Interestingly the lysine alpha-beta cross peaks which was not resolved in the EK5 peptide, were clearly visible in the spectrum of

the EK3.3a peptide at 1.8, 4.2ppm. This may also be attributable to a more stable conformation of the EK3.3a peptide.

One dimensional spectra of the EK3.3a and EK4.0 peptide were acquired at NYU (Appendix 4.1 4.2.1). Interpretation of these spectra is difficult due to peak overlap. The two spectra appear very similar which may be evidence that the two proteins are in similar conformations. The amide proton regions of both peptides are well resolved and show several distinct doublets; interpretation of the coupling in this region may be possible and could be possible confirmation of helicity. The alpha proton region of the EK3.3a peptide shows three broad peaks, while this region of the EK4.0 peptide shows only one broad peak. This may be due, in part, to the three different sections of salt bridging in the EK3.3a peptide (C-terminus $i,i+3$, $i,i+4$, and N-terminus $i,i+3$) as compared with three section of $i,i+4$ salt bridging of the EK4.0 peptide. A 1-D spectrum of the EK3.3a peptide in D_2O taken on the Gemini 200 (Appendix 4.2.2) also showed these three alpha peaks. 1-D spectra of the EK4.0 peptide were not taken at 200MHz due to time limitations and the lower solubility of the EK4.0 peptide.

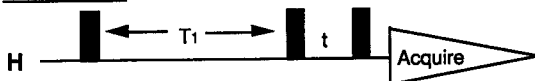
Figure 3.3 Pulse Sequences

COSY



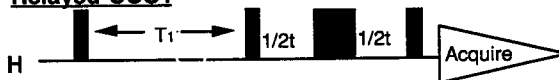
Pros: Resolves bond connectivities and peak overlap.
Cons: Poor resolution. Broad diagonal can obscure peaks.

DQF-COSY



Pros: Allows greater resolution, and separation of the diagonal.
Cons: Slightly lower sensitivity.

Relayed-COSY



Pros: Allows resolution of overlapped peaks and confirmation of connectivities, highly selective.
Cons: Slightly lower sensitivity and lack of generality.

NOESY



Pros: Shows spatial relationships.
Cons: Extremely low sensitivity. Highly sensitive to mixing time.

TOCSY/HOHAHA



Pros: Resolution of overlapped regions. Particularly useful in assignment in peptides and proteins.
Cons: Slightly low sensitivity.

Chapter 4

Conclusion & Future Research

COMPUTER MODELING

It is difficult to make definitive statements about the total helicity of the EK3.3 and EK4.0 peptides due to the limited nature of our models. However, they do provide useful insight into possible interactions of the peptides. The models show the predicted salt bridging and provide one explanation for observed aggregation. The accuracy of these predictions should be determined from future experimental data.

Future Modeling

In order to refine the current models, future modeling should include different starting conformations of the EK4.0 and EK3.3 peptides. Further iterations of current model EK4.0 peptide should also be carried out to determine reliable energy minima. A comparison of the values derived from energy minimization calculation and the experimentally determined percent helicity could provide useful insight into the accuracy of these relatively simple models. Studies of an all $i,i+3$ salt bridged peptide and the inverse peptide to the EK3.3 peptide (e.g. the EK3.7 peptide with $i,i+4$, $i,i+3$, $i,i+4$ salt bridging) would also provide interesting comparisons.

5-MER NMR STUDIES

It is possible to obtain nearly complete assignments the chemical shift of a small peptide with a limited number of the same type of amino acids. However, the two dimensional experiments used do not allow complete resolution of two amino acids of the same type in a single peptide. Further, current instrument setup lacks the needed sensitivity to resolve certain weak multiplets.

It is impossible to make any definitive statements about the conformation of the EK5 peptide at any pD as it was not possible to obtain any of the needed conformational constraints. It is reasonable to assume, based on the available evidence, that there are some changes in the peptide at various pH. However, how or if these changes correspond to conformational changes cannot be definitively determined.

Future Research

Low temperature studies of the peptide could provide information on whether the peptide is in several rapidly converting different conformations. However, such studies may have limited application and should be deferred in favor of exploring the use of experiments which would have more general application to other NMR studies.

The first priority of future research should be to determine the best parameters for conducting experiments in water. It may be necessary to increase H₂O/D₂O ratios to 50/50 due to limitations of the decoupler to provide power to saturate the water signal. It is not known if design of the current probe will play a role in the success of any future NMR water spectra. Future communication with Varian should be most helpful in this area.

The availability of water spectra will prove helpful in any future peptide experiments. The broad range of amide protons may allow resolution of the two alanine alpha protons which are not resolved in the D₂O experiments. The resolution of the 200 MHz instrument may be sufficient to allow study of the deuterium exchange rates in an appropriately designed helical peptide such as described by Zhou, Hull and Kallenbach³⁴.

The possible use of the TOCSY experiment with the Gemini 200 should also be explored. The TOCSY experiment requires a probe capable of generating a sustained strong pulse for a durations of several 100ms. This capability will be the limiting factor in the use of this experiment in the Gemini 200. If it is possible to use this experiment with the current setup of the instrument, the pulse sequence should be available from Varian. Should the use of the TOCSY experiment prove unfeasible in the Gemini 200, it should be possible to correlate amide protons to beta protons through the use of relayed and double relayed experiments³² of the type introduced on the instrument in this research.

In the future, use of a probe designed for direct proton detection could vastly improve the sensitivity of this instrument and its application to studies of small peptides. The use of imaging software such as "Felix" could greatly improve the ease with which experiments are interpreted as well as providing improved algorithms for resolution and sensitivity enhancement. Increased spectrometer memory capabilities will also allow improvements in sensitivity and resolution through the use of larger experiments with a greater number of t_1 increments and a larger number of transients.

18-MER NMR STUDIES

The NOESY spectrum of the EK3.3 peptide shows several intra residue NOEs suggesting that the peptide has at least one stable confirmation. Any stable conformations of the EK3.3 and EK4.0 peptides are likely helical due their design. Further, one dimensional experiments on the EK3.3 and EK4.0 peptides are quite similar, thus it is likely that both peptides are in similar

helical conformations. However, this is not definitive evidence of helicity. Future analyses of the spectra is necessary to confirm helicity.

Future Research

Interpretation of the NMR spectra of the EK3.3 peptide should provide information on the helical structure of the peptide. Such information should include the relative helicity and structure of any helix present in different sections of the peptide. It maybe also be possible to determine if the side chains of the lysine and glutamic acid are in close proximity from interpretation of NOEs. This could provide good evidence for stabilization of the these helices though side chain interactions.

Future NMR experiments on these peptides should include a one-dimensional spectrum of the purified peptides to determine the accuracy of the chemical shift assignment from the unpurified spectra. New NOESY experiments should also be acquired in order to eliminate the possibility of any conformational effects from contaminates. Temperature NMR studies might also provide information on differences in the helical structure of the peptides at low temperature.

OTHER FUTURE STUDIES

CD experiments must be performed in order to determine that there are no conformational effects on the helicity of the peptides at the concentrations studied by NMR. NMR experiments will not give quantitative evidence for the percent helicity of each peptide, therefore, it is important that the percent helicity of each peptide be determined by CD. This is especially important in the case of the EK4.0 peptide where useful NMR information is unlikely to be obtained. CD experiments should be conducted

to determine the dependence of helicity on pH and the percent helicity of the peptides at the pH studied by NMR. These pH studies will be important in proving that the peptides are being stabilized by salt bridge interactions. Temperature studies of the peptides should be carried out by CD to determine the stability of the helix. All of these experiments are important indications of the helix stability of the peptide. These studies combined with the NMR data should provide definitive evidence for the structure of the EK4.0 and EK3.3 peptides.

REFERENCES

UN82

ERNST, J. NMR STUDIES OF SHORT SALT BRIDGED PEPTIDES

E73n/1994

DEPARTMENT OF CHEMISTRY HRS. 6/94

2/2



- (1) IUPAC-IUB; Commission on Biochemical Nomenclature, *Biochemistry*. 1970, 9, 3471.
- (2) Pauling, L.; Corey, R. B.; Bronson, H. R. *Proc. Natl Acad. Sci. USA*. 1951, 37, 205.
- (3) (a) Barlow, D. J.; Thornton, J. M. *J. Mol. Bio.* 1988, 201, 601.
 (b) Richardson, J. S.; Richardson, D. C. *Science*. 1988, 240, 1648.
 (c) Fasman, G. D. *Prediction and Protein Structure and the Principles of Protein Conformation*; Plenum Press, New York, 1991, 193-316.
- (4) (a) Roder, H.; Elove, G.; Englander, S. W. *Nature*. 1988, 335, 700.
 (b) Englander, S. W.; Mayne, L. *Annu. Rev. Biophys. Bio.* 1992, 21, 243.
 (c) Lu, L.; Dahlquist, F. W. *Biochemistry*. 1992, 31, 4749.
 (d) Baldwin, R. L. *Curr. Opin. Struct. Bio.* 1993, 3, 84.
- (5) Fiori, R.W.; Mück, M. M.; Millhauser, G. L. *Biochemistry*. 1993, 32, 11957-11962.
- (6) Dickerson, R. E.; Giels, I. *The Structure and Action of Proteins*, Harper & Row, New York, 1969.
- (7) (a) Scholtz, J. M., Baldwin, R. L. *Annu. Rev. Biophys. Biomol. Struct.* 1993, 21, 95.
 (b) Marqusee, S.; Baldwin, R. L. *Proc. Natl. Acad. Sci. USA*. 1987, 84, 8898.
- (8) Poland, D.; Scheraga, H. A. *Academic press*, New York, 1970.
- (9) (a) DeGrado, W. F.; O'Neil, K. T. *Science*, 1990, 250, 646.
 (b) Chakrabarty, A.; Schellman, J. A.; Baldwin, R. *Nature*. 1991, 352, 586.
 (c) Merutka, G.; Stellwagen, E., *Biochemistry*, 1990, vol 29, 894-898. 250, 669-973.
 (e) Padmanabhan, S.; Marqusee, S.; Ridgeway, T.; Laue T. M.; Baldwin, R. L., *Nature*. 1990, 344, 268.
- (10) Huyghues-Despointes, B. M.P.; Scholtz, M.; Baldwin, R. L. *Protein Science*. 1993, 2, 80.
- (12) Marqusee, S.; Robbins, V. H.; Baldwin, R. L. *Proc. Natl. Acad. Sci. USA*. 1989, 86, 5286-5290.
- (13) Jones, J. *Amino Acid And Peptide Synthesis*, Oxford, New York, 1992.
- (14) Liff, I. M.; Kallenbeck N. R. *J. Am. Chem. Soc.* 1991, 113, 1014

- (15) Wuthrich, K. *NMR of Proteins and Nucleic Acids*. Wiley, New York 1986.
- (16) Bystrov, V. F. *Progress in NMR Spec.* 1979, 10, 41.
- (17) Piantini, U.; Sorensen, O.W.; Ernst, R. R. *J. Am. Chem. Soc.* 1982, 104, 6801.
- (18) Neuhaus D.; Williamson M. *The Nuclear Overhauser Effect in structural and Conformational Analysis*, VCH, New York, 1989.
- (19) Wuthrich, K.; Billeter, M.; Braun, W. *J. Mol. Biol.* 1984, 180, 715.
- (20) (a) Braunschweiler, L.; Ernst, R.R. *J. Magn. Reson.* 1983, 53, 521.
(b) Bax, A.; Davis, D. *J. Magn. Reson.* 1985, 65, 355.
- (21) Paridi, A.; Wagner, G.; Wuthrich, K. *Eur. J. Biochem.* 1983, 137, 445.
- (22) Kollman, P. *Ann. Rev. Phys. Chem.* 1987, 38, 303.
- (23) Mohamadi, F; et al. *J. Comp. Chem.* 1989, 11, 440.
- (24) McCammon, J.A.; Harvey, S.C. *Dynamics of protein and nucleic Acids*. Cambridge, New York 1987.
- (25) Weiner, S.; Kollman, P. A; et al. *J. Am Chem Soc.* 1984, 106, 765.
- (26) Stewart, J. M., Young, J. D. *Solid Phase Peptide Synthesis*, 2nd ed.; Pierce Chemical Co, Illinois 1984; 105-107.
- (27) King, D. S.; Fields, G. C.; Fields, B. G. *Int. J. Pep. Pro. Res.*, 1990, 36, 255-266.
- (28) Berger, S. J. *Synthesis of a Hybrid Baldwin Peptide: A Study in Factors that Influence Helix Formation*, Union College, Schenectedy, NY, 1984
- (29) Derome, A. E. *Modern NMR Techniques for Chemistry Research*, Pergamon, New York, 1987.
- (30) Bax, A. *Two Dimensional Nuclear Magnetic Resonance in Liquids*, Delf, Dordrecht, 1982.
- (31) Fukushima, E., Stephen, B. W. R. *Experimental Pulse NMR A Nuts and Bolts Approach*, Addison-Wesley, Reading, MA, 1981.

- (32) (a) Wagner, G. *J. Mag. Res.* **1983**, 55, 151-156.
(b) Bax, A.; Drobny, G. *J. Mag. Res.* **1985**, 61, 306-320.
- (33) Clore, G. M.; Gronenborn, A. M. *Ann Rev. Biophys. Biochem.* **1991**, 20, 29-63.
- (34) Zhou, H. X.; Hull, L. A.; Kallenbach, R. N. *accepted J. Am. Chem. Soc.*

Appendix 1
Computer Modeling

Appendix 1.1 MacroModel .com File For The Model EK4.0 Peptide

```
$setdef <main directory>
$run [<main directory>.macromodel.mmv30.inc1]BATCHMIN
ek40.dat
ek40.out
FFLD 3 1.0000
SOLV 3 1 10 0
READ
CONV 1 0.01
MINI 1 0 25000
MMOD
ELST 01
```

Appendix 1.2 MacroModel Output File for the Model EK4.0 Peptide

Energy Equations in Use:

Bond Length - 1: Harmonic stretch
Bond Angle - 1: Harmonic bend
Stretch-Bend - 0: None
Torsional - 1: 1-3 Fold cosine function
Improper Torsion (OPB) - 2: Improper torsion
Van der Waals - 2: Softcut 6,12-Lennard Jones (R,Eps)
1,4-Van der Waals - 3: multiplier 0.50
1,4-Electrostatics - 3: multiplier 0.50
Electrostatic - 1: Point charge with constant dielectric
Hydrogen-Bonding - 1: Angle-independent 10,12-Lennard Jones
Fixed Atoms - 1: Harmonic anchoring
Angular H-Bonds (A-B-C) - 0: None
Angular H-Bonds (A-B-C-D) - 0: None
Solvation Model - 3: GB/SA Solvation
Solvent is WATER

Alternative parameter sets selected:

Number	Label	Description
1	"b"	United atom field charges
2	"z"	Zinc

Parameter qualifier sets selected:

Column	Label	Description
1	"O"	Original AMBER params
1	"M"	Modified params
1	"A"	Added params
2	"1"	Specific, high quality params
2	"2"	Tentative values for params
2	"3"	Generalized, low quality param

Total amber.fld energy is -4045.843 kJ/mol (-966.980 kcal/mol)

Van der Waals -153.762 (-36.750) Stretch 8.136
Torsion 32.485 (7.764) Bend18.819

Improper Torsion 0.846 (0.202) Stretch-Bend 0.000
Hydrogen Bond -31.168 (-7.449) Electrostatic -2587.344 (-61)

Appendix 1.2con.

MacroModel Output File For The Model EK4.0 Peptide

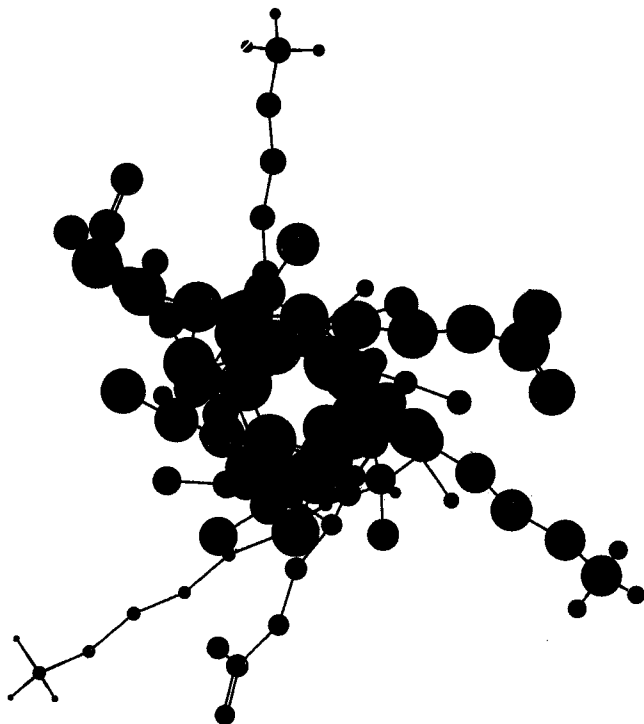
Solvation Term 1 45.421 (10.856)
Solvation Term 2 -1379.275 (-329.655)
Solvation Term 3 0.000 (0.000)
Dipole moment of total system = 8.830 debyes

Maximum van der Waals distance = 7.0 Angstroms
Maximum electrostatic distance = 12.0 Angstroms
Maximum hydrogen bond distance = 4.0 Angstroms
Molecular dielectric constant = 1.00
Solvent dielectric constant = 78.30

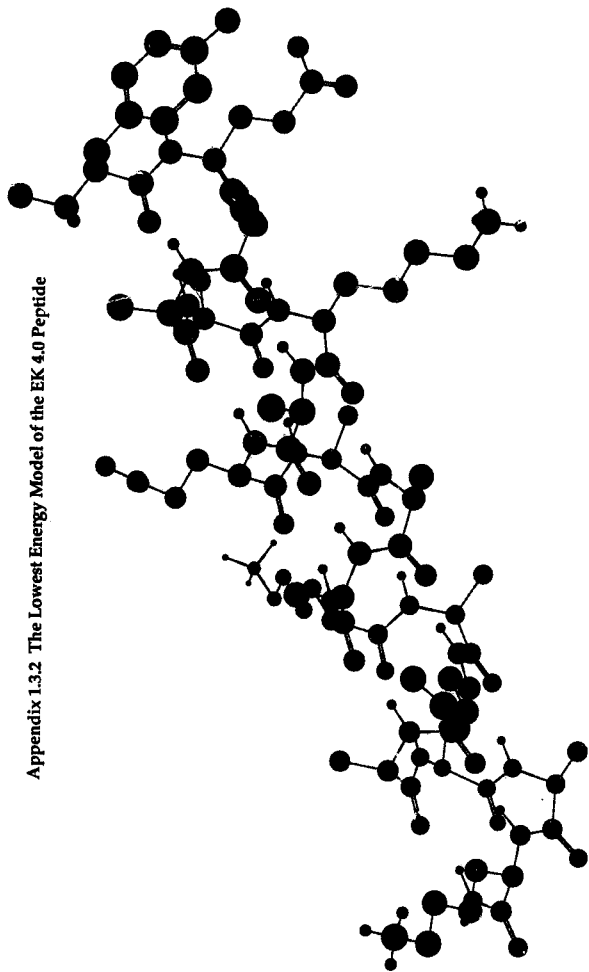
RMS Gradient = 1.7988 kj/A-mol

CPU Time = 4363.35 seconds

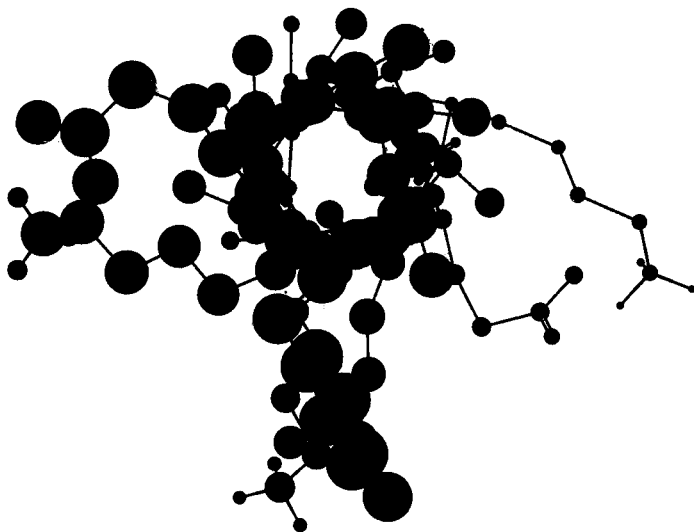
Appendix 1.3.1 The Lowest Energy Model of the EK 4.0 Peptide



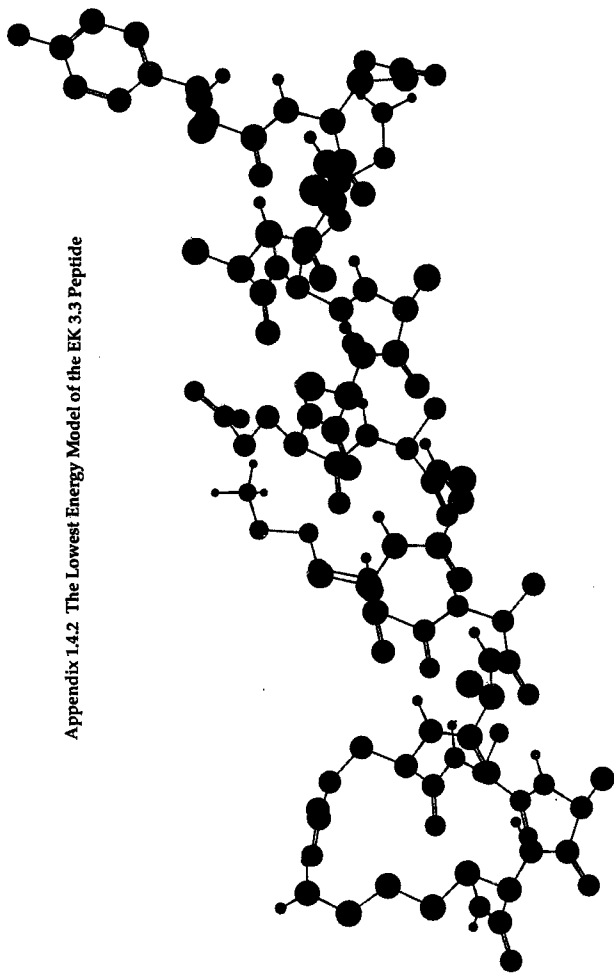
Appendix 1.3.2 The Lowest Energy Model of the EK 4.0 Peptide



Appendix 1.4.1 The Lowest Energy Model of the EK 3.3 Peptide

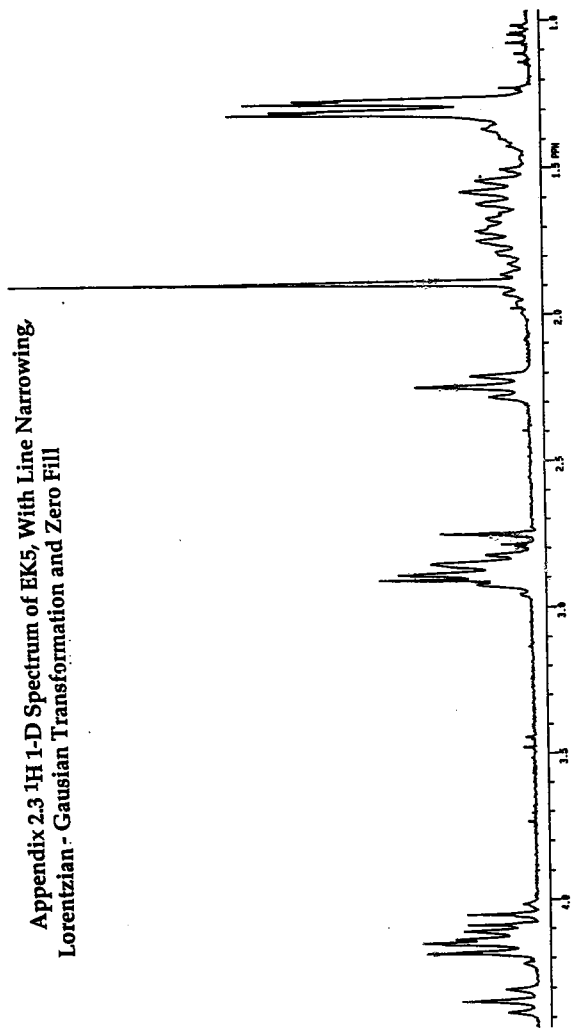


Appendix 1.4.2 The Lowest Energy Model of the EK 3.3 Peptide

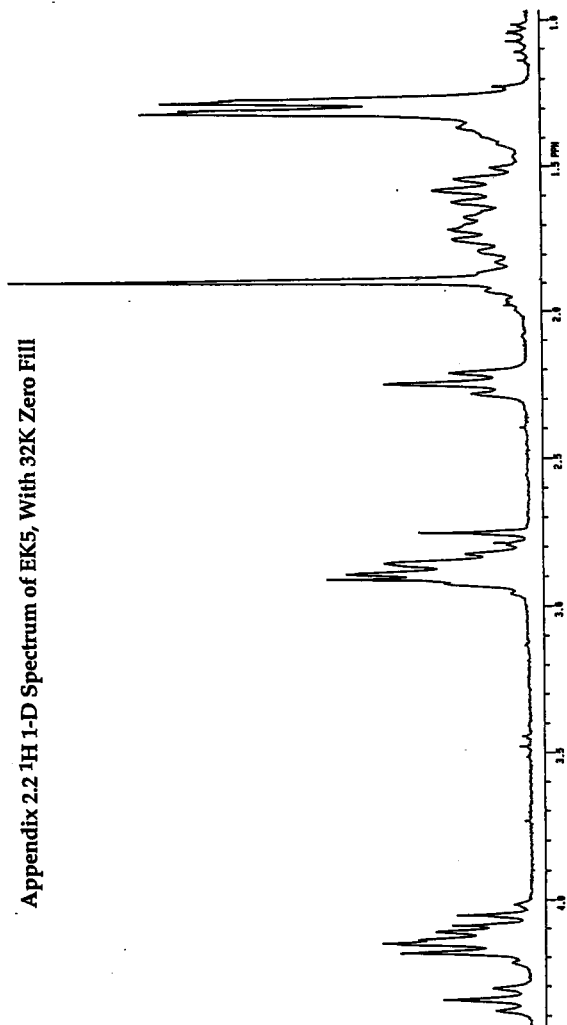


Appendix 2
Resolution Enhancement

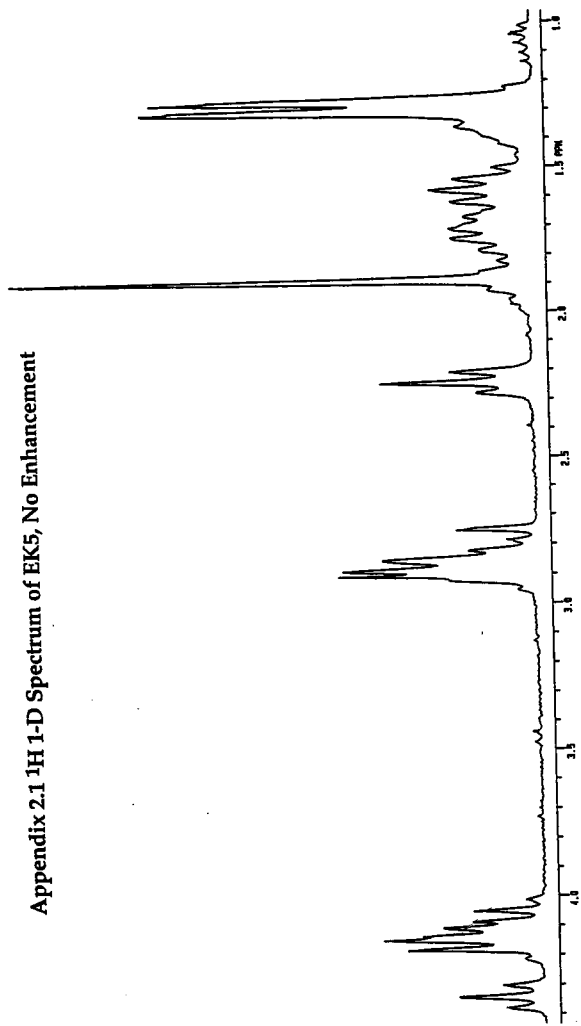
**Appendix 2.3 ^1H 1-D Spectrum of EK5, With Line Narrowing,
Lorentzian - Gaussian Transformation and Zero Fill**



Appendix 2.2 ^1H 1-D Spectrum of EK5, With 32K Zero Fill

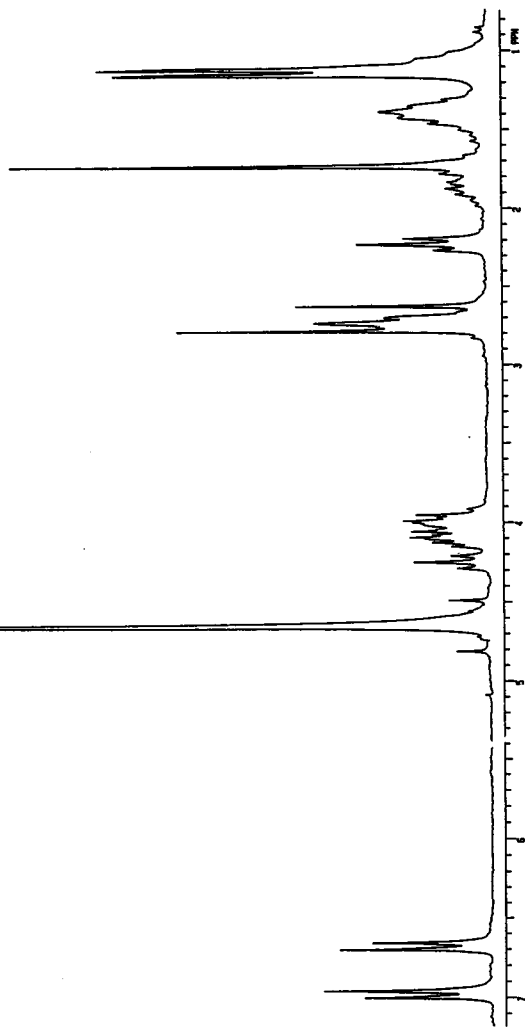


Appendix 2.1 ^1H 1-D Spectrum of EK5, No Enhancement

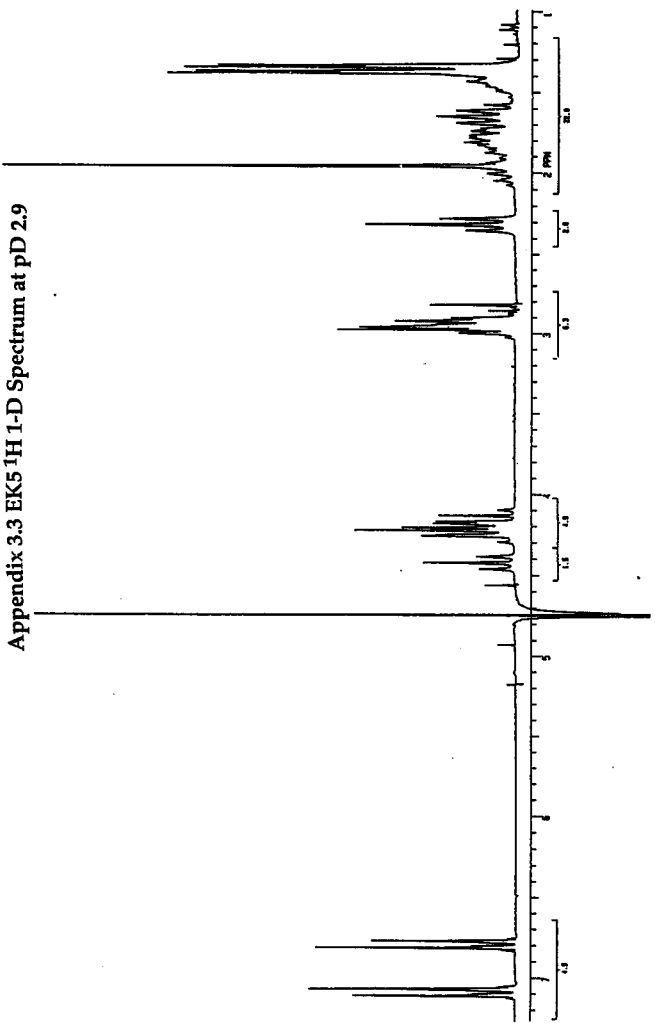


Appendix 3
NMR Spectra of the 5-Mer Peptides

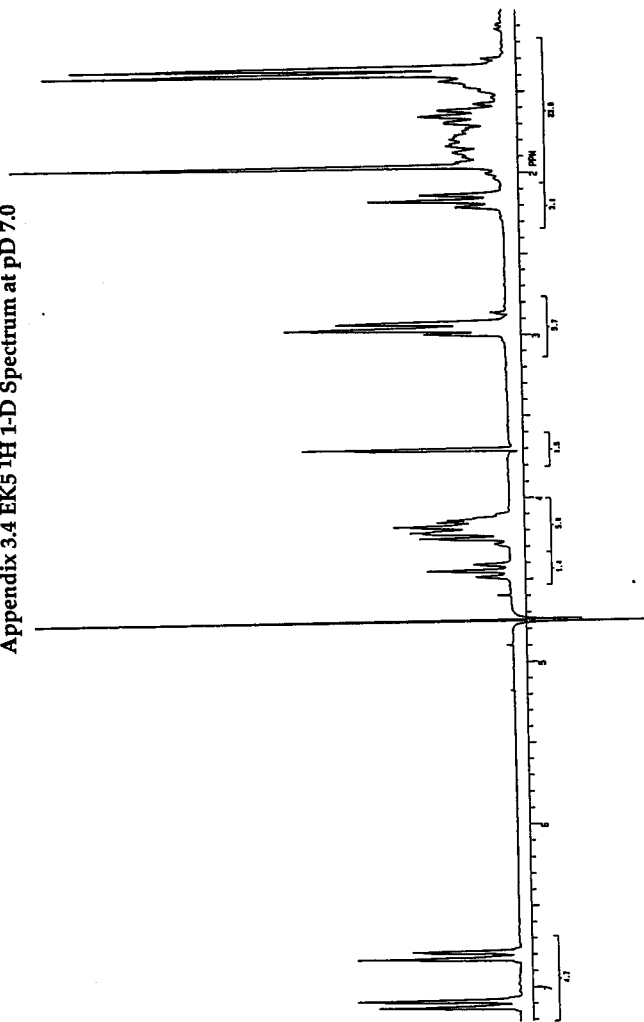
Appendix 3.1 KE5 1H 1-D Spectrum at pD 2.9



Appendix 3.3 EK5 ¹H 1-D Spectrum at pD 2.9

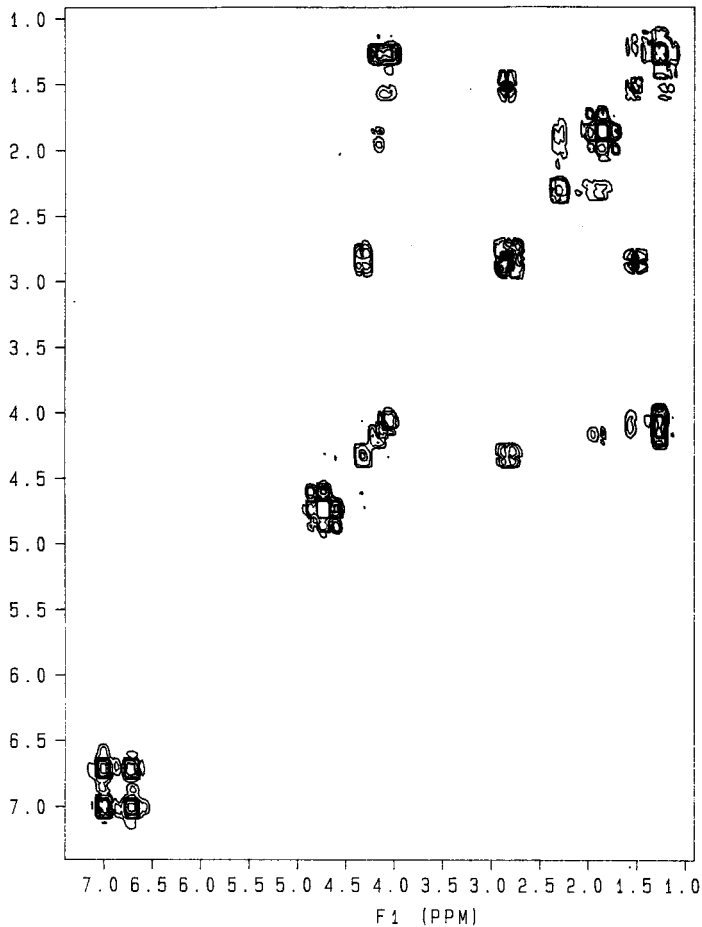


Appendix 3.4 EK5 1H 1-D Spectrum at pD 7.0

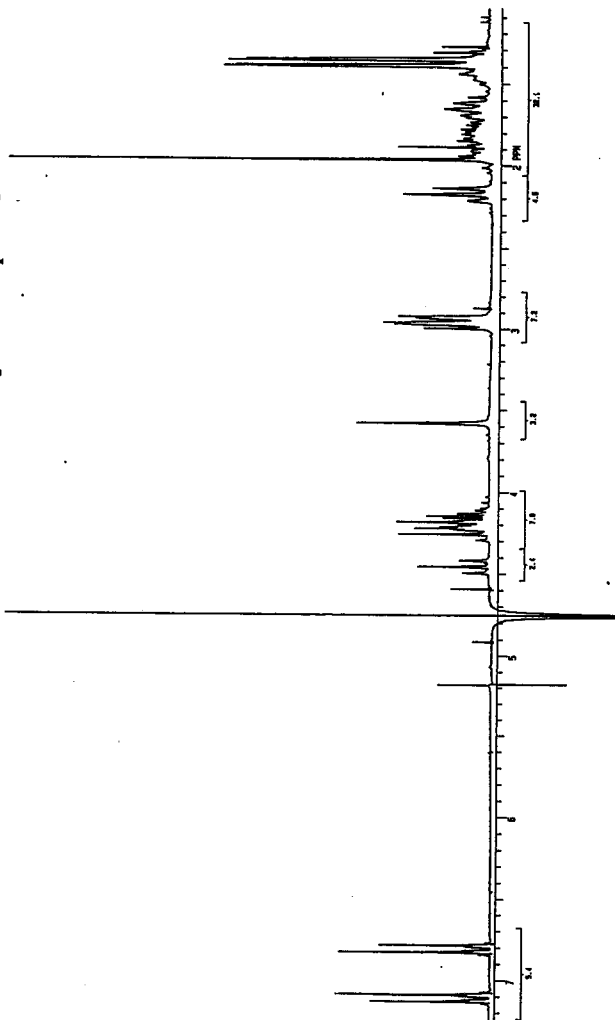


F2 (PPM)

Appendix 3.2 KE5 ¹H COSY at pD2.9

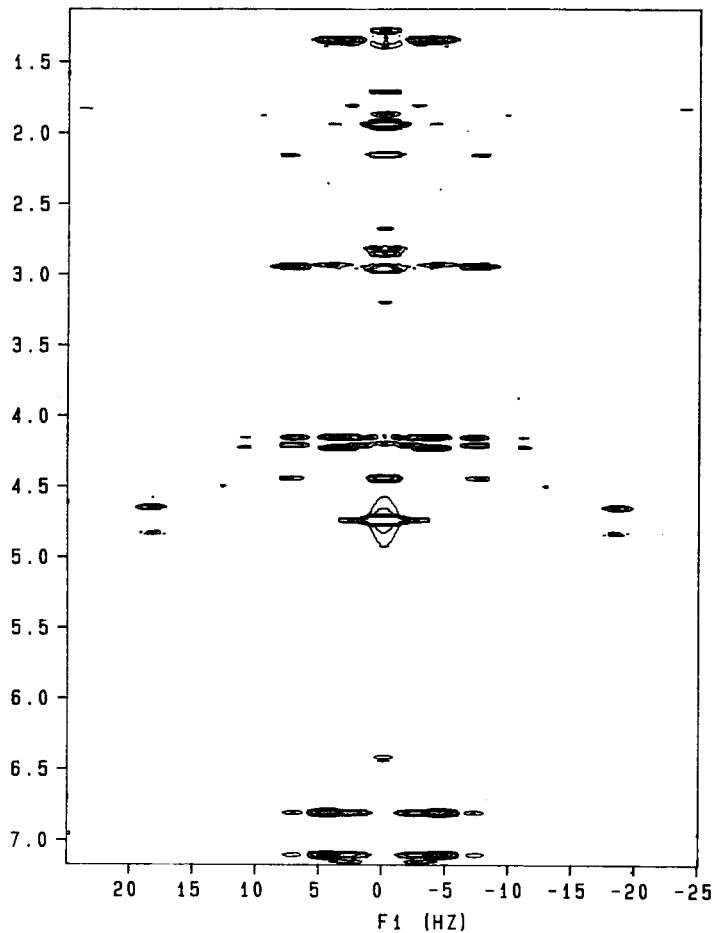


Appendix 3.5 EK5 1H 1-D Spectrum at pD 11.3



F2 (PPM)

Appendix 3.6 EK5 ^1H -J-Resolved pD 7.0

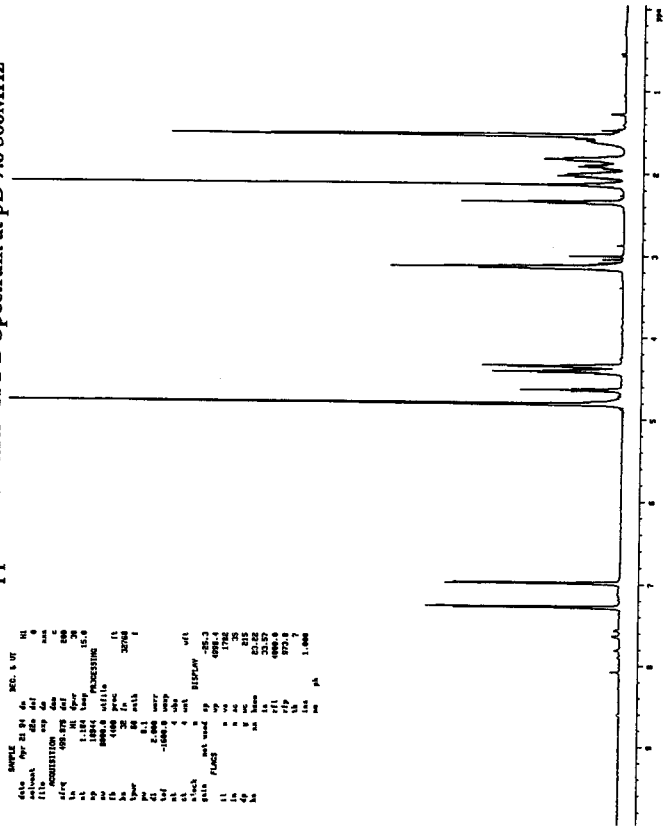


EX-
Spectroflashing Sw

expd pulse sequence (ppm)

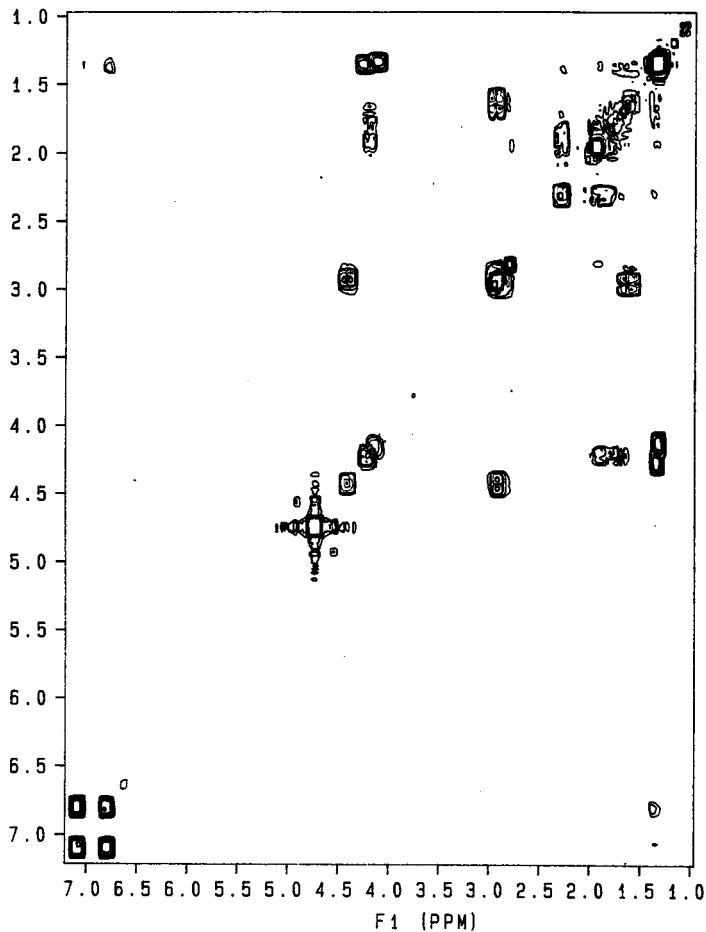
6146 Ppt 21.24 46 300.15 Vt N1
 calcont 0 0 0
 ITCONSISTION 50 50 0 0 0
 4174 084.770 4d 0 0 0
 41 1.150 4d 0 0 0
 44 1.150 4d 0 0 0
 49 1.004 POLYESTER
 46 1.004 POLYESTER
 51 1.004 POLYESTER
 56 2.31 0 0 0
 53 2.31 0 0 0
 52 6.1 0 0 0
 54 -10.000 0 0 0
 55 -10.000 0 0 0
 57 1.004 0 0 0
 58 1.004 0 0 0
 59 1.004 0 0 0
 60 1.004 0 0 0
 61 1.004 0 0 0
 62 1.004 0 0 0
 63 1.004 0 0 0
 64 1.004 0 0 0
 65 1.004 0 0 0
 66 1.004 0 0 0
 67 1.004 0 0 0
 68 1.004 0 0 0
 69 1.004 0 0 0
 70 1.004 0 0 0
 71 1.004 0 0 0
 72 1.004 0 0 0
 73 1.004 0 0 0
 74 1.004 0 0 0
 75 1.004 0 0 0
 76 1.004 0 0 0
 77 1.004 0 0 0
 78 1.004 0 0 0
 79 1.004 0 0 0
 80 1.004 0 0 0
 81 1.004 0 0 0
 82 1.004 0 0 0
 83 1.004 0 0 0
 84 1.004 0 0 0
 85 1.004 0 0 0
 86 1.004 0 0 0
 87 1.004 0 0 0
 88 1.004 0 0 0
 89 1.004 0 0 0
 90 1.004 0 0 0
 91 1.004 0 0 0
 92 1.004 0 0 0
 93 1.004 0 0 0
 94 1.004 0 0 0
 95 1.004 0 0 0
 96 1.004 0 0 0
 97 1.004 0 0 0
 98 1.004 0 0 0
 99 1.004 0 0 0
 100 1.004 0 0 0

Appendix 3.7 EK5 IH 1-D Spectrum at pD 7.0 500MHz



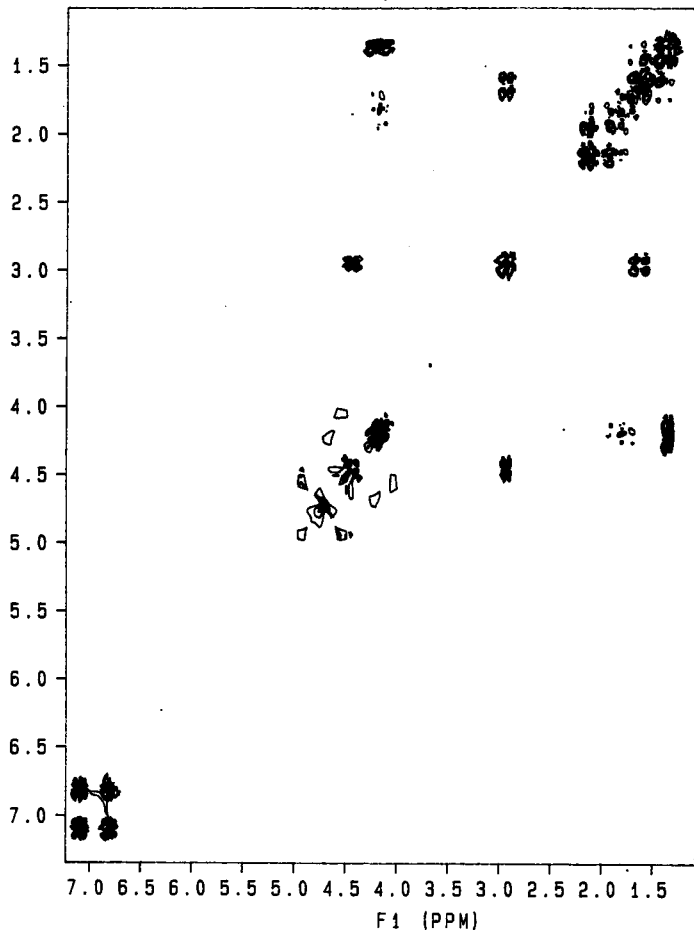
F2 (PPM)

Appendix 3.8 EK5 ¹H COSY pD3

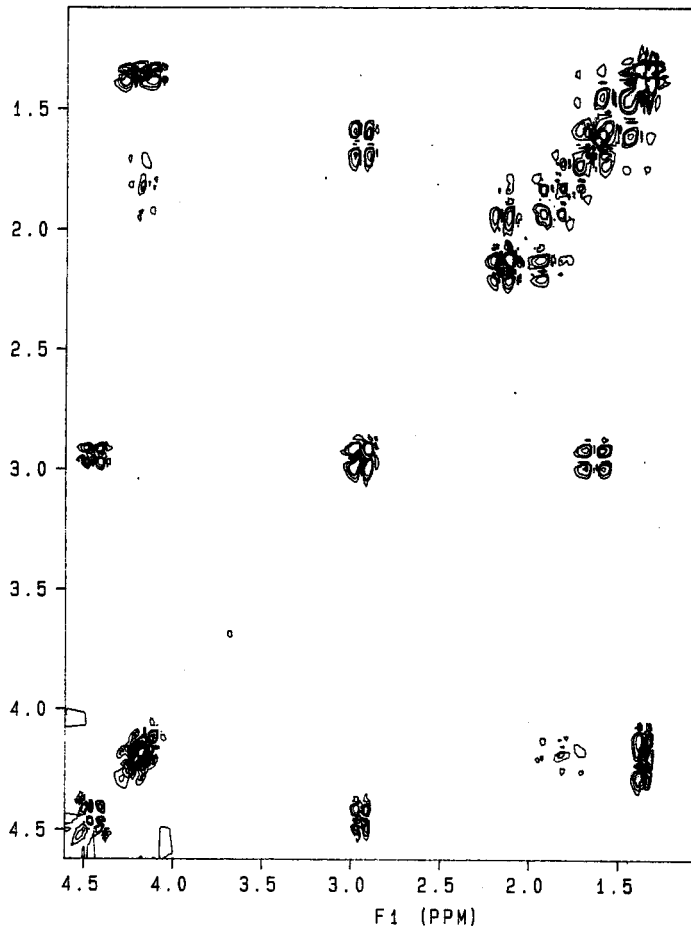


F2 (PPM)

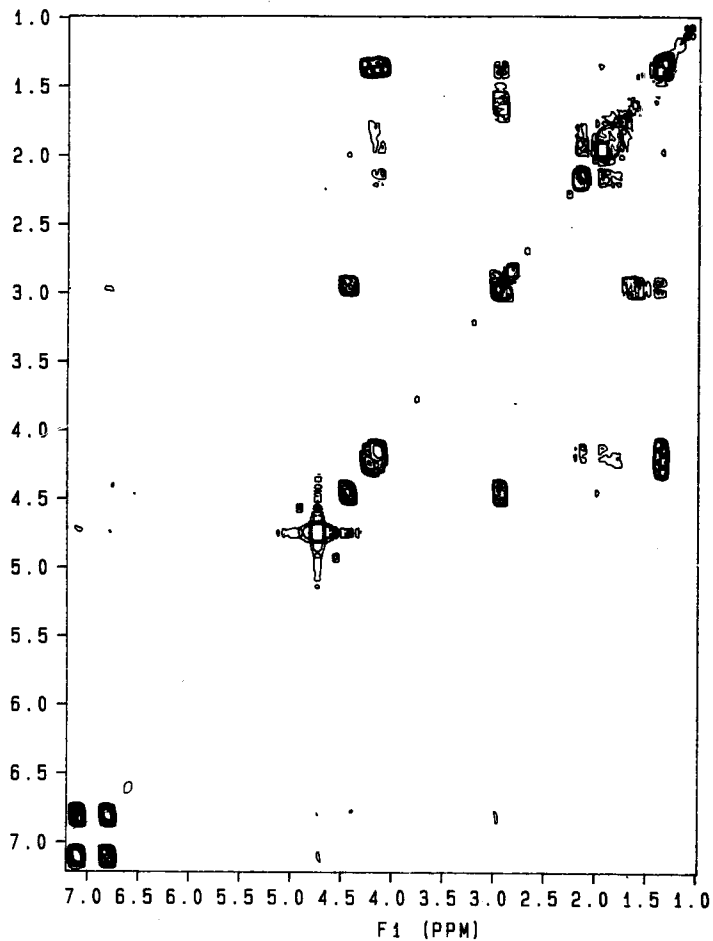
Appendix 3.9.1 EK5 ^1H DQF-COSY pD 7.0
Non-spinning Sample



Appendix 3.9.2 EK5 ^1H DQF-COSY pD 7.0 Expanded Region
F2 (PPM) Non-spinning Sample

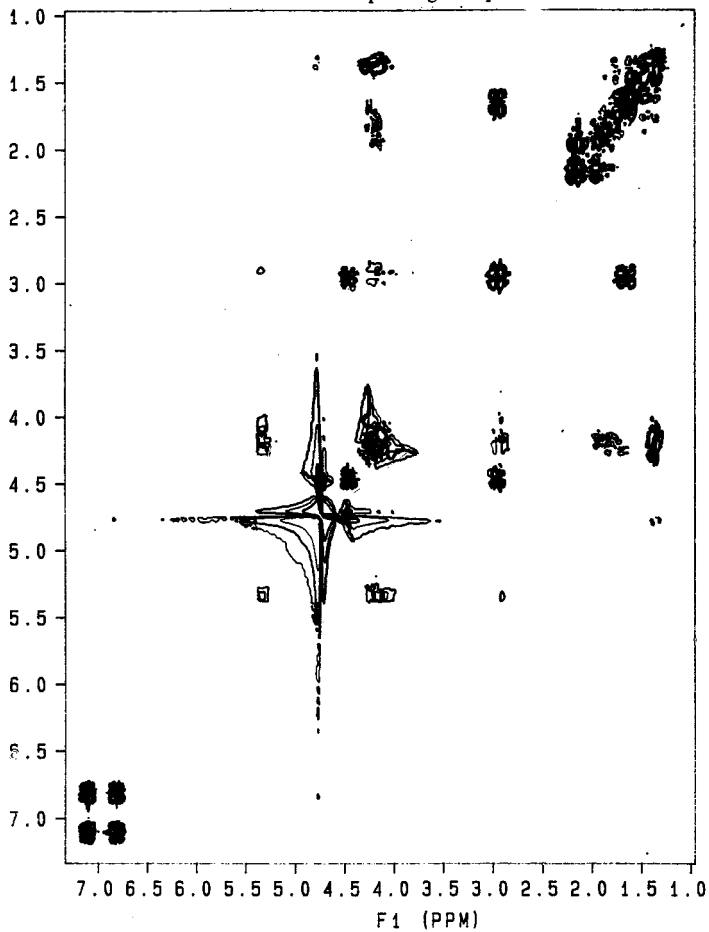


F2 (PPM) Appendix 3.10 EK5 ¹H Relayed COSY pD 7.0 τ = 35ms



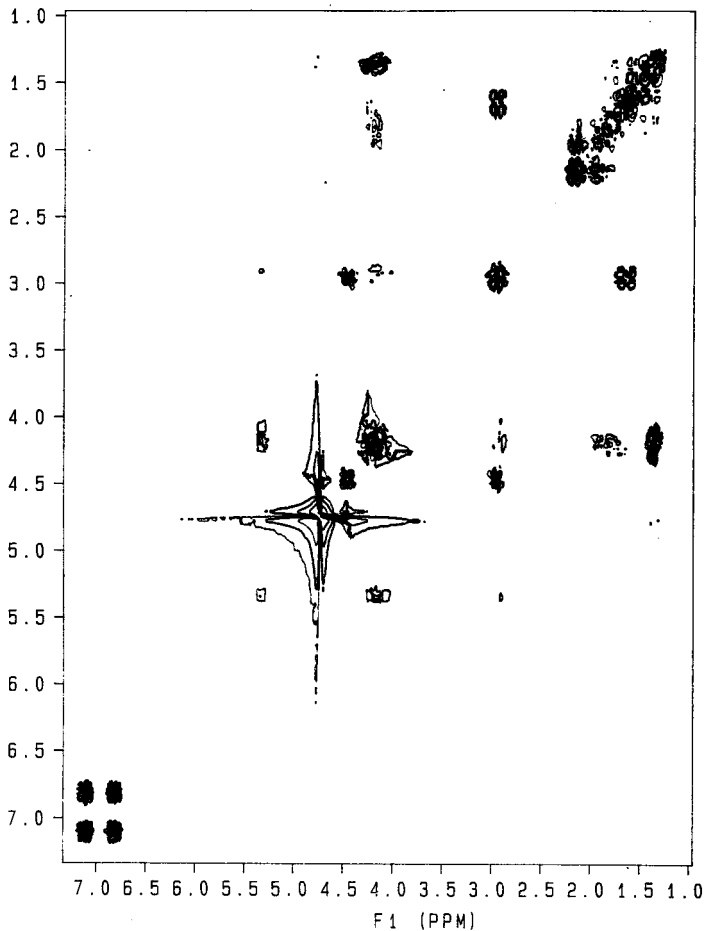
F2 (PPM)

Appendix 3.11.1 EK5 ^1H DQF-COSY pD 11.3,
Non-spinning Sample

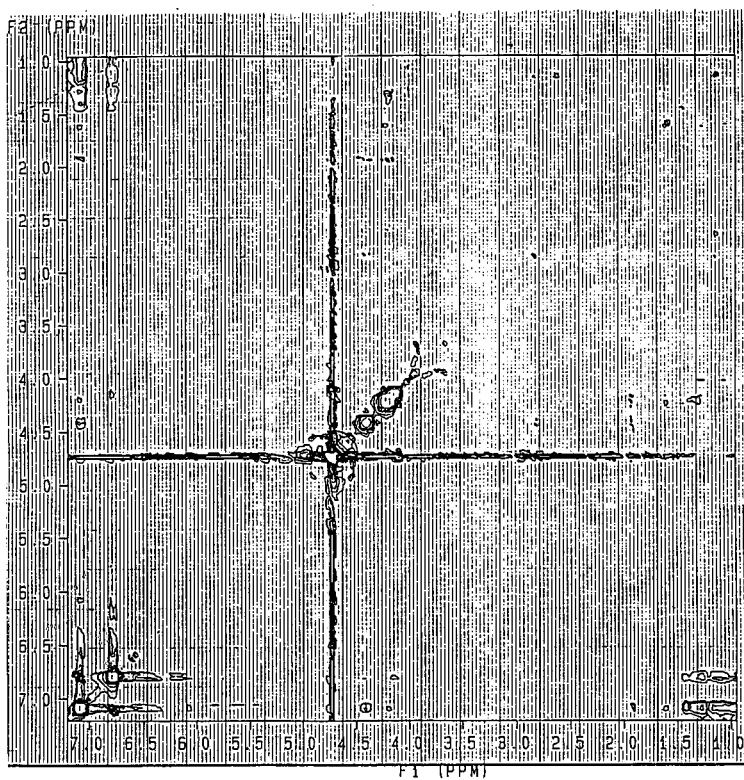


F2 (PPM)

Appendix 3.11.2 EK5 ^1H DQF-COSY pD 11.3,
Spinning Sample



Appendix 3.12 EK5 NOESY pD 2.9 200 ms mixing time



Appendix 4
NMR Studies of the 18-mer Peptides

Appendix 4.2.1 EK3.3 1H 1-D Spectrum at pH 5.5 500 MHz

023.3
 spector: Magnetom Bruker
 exp# 0116 acquisition: 0116

NAME: EK3.3
 EXPNO: 3
 PROCNO: 3
 F2 - Acquisition Date: 19990804

PROBHD: zgpg30
 PULPROG: zgpg30
 CHANNEL: 1h
 NUC1: 1H
 FREQ: 500.137

NUC2: 13C
 FREQ2: 125.763
 AQC: 10.00
 SFO: 500.136450
 AQS: 10.00
 ASFO: 125.762500

TD: 65536
 SCA: 32768
 SCALFA: 2.000000
 SCALF2: 2.000000
 SCALF3: 2.000000

RG: 512
 RGA: 256
 RGF: 256
 RGD: 256
 RGX: 128
 RGY: 128

SI: 32768
 SF: 500.136450
 SF2: 125.762500
 SF3: 20.000000
 SF4: 20.000000

WDW: EM
 SSF: 0.00
 GB: 0.00
 PC: 1.00
 SC: 0.00
 RC: 0.00

LB: 3.00
 LB2: 3.00
 LB3: 3.00
 LB4: 3.00
 LB5: 3.00

GB2: 0.00
 GB3: 0.00
 GB4: 0.00
 GB5: 0.00
 GB6: 0.00

PC2: 1.00
 PC3: 1.00
 PC4: 1.00
 PC5: 1.00
 PC6: 1.00

SC2: 2.00
 SC3: 2.00
 SC4: 2.00
 SC5: 2.00
 SC6: 2.00

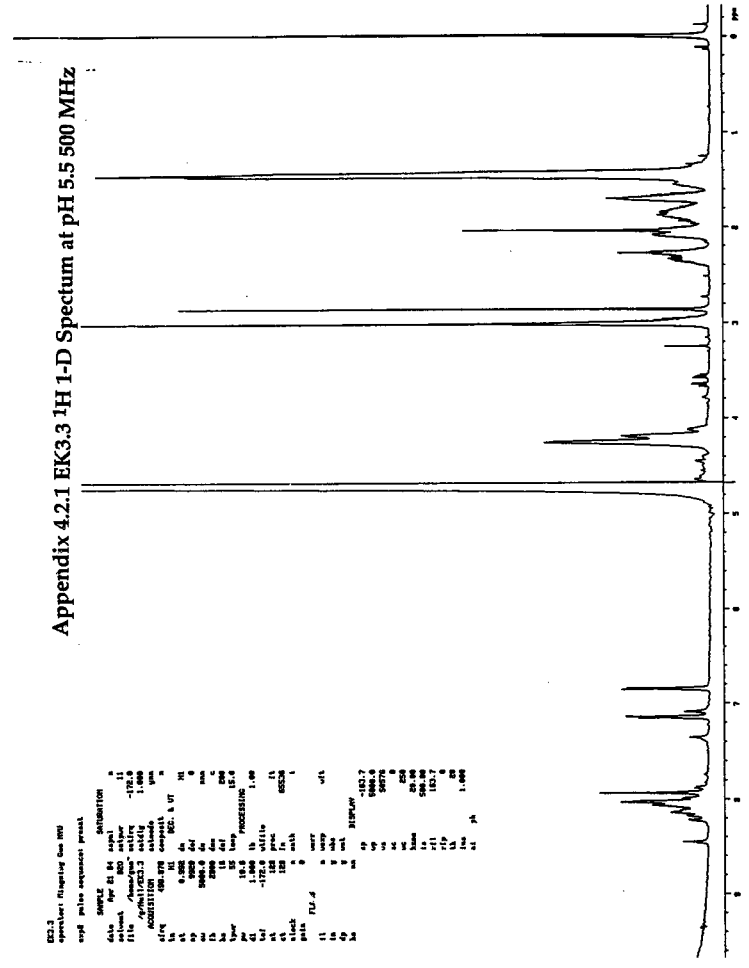
WDW2: EM
 WDW3: EM
 WDW4: EM
 WDW5: EM
 WDW6: EM

SSB: 0
 SSB2: 0
 SSB3: 0
 SSB4: 0
 SSB5: 0

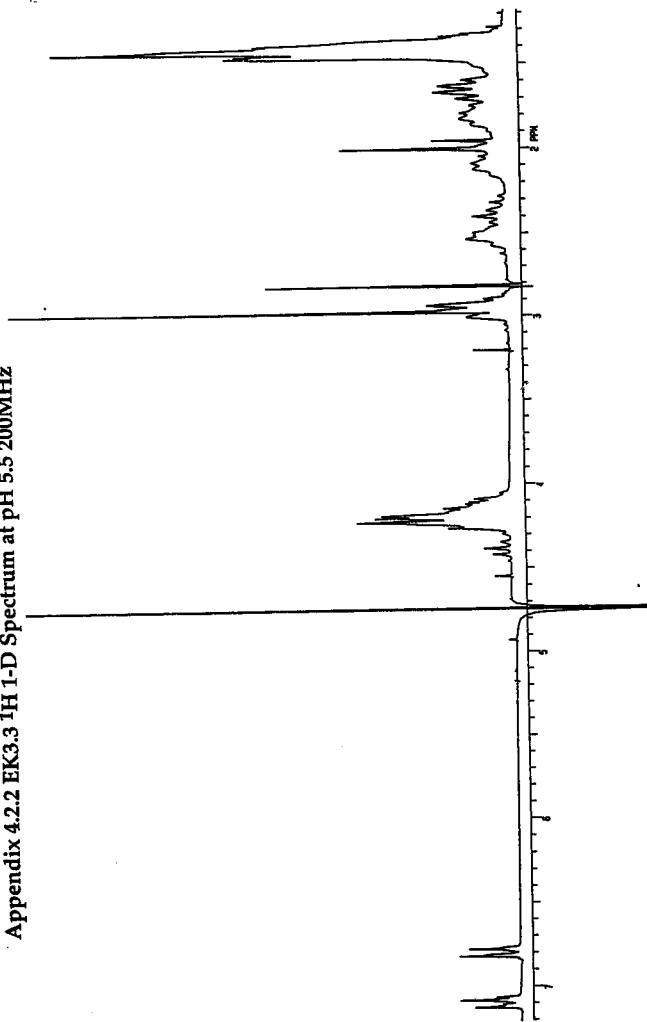
SSB6: 0
 SSB7: 0
 SSB8: 0
 SSB9: 0
 SSB10: 0

SSB11: 0
 SSB12: 0
 SSB13: 0
 SSB14: 0
 SSB15: 0

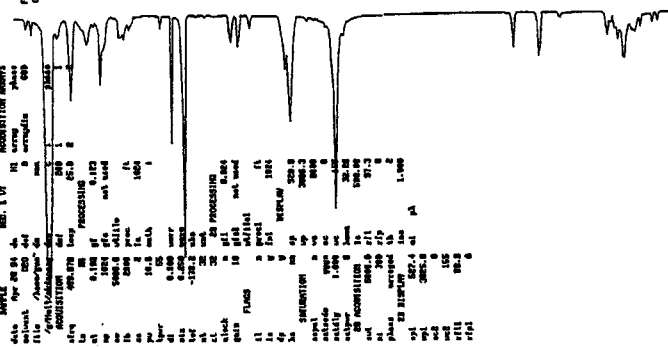
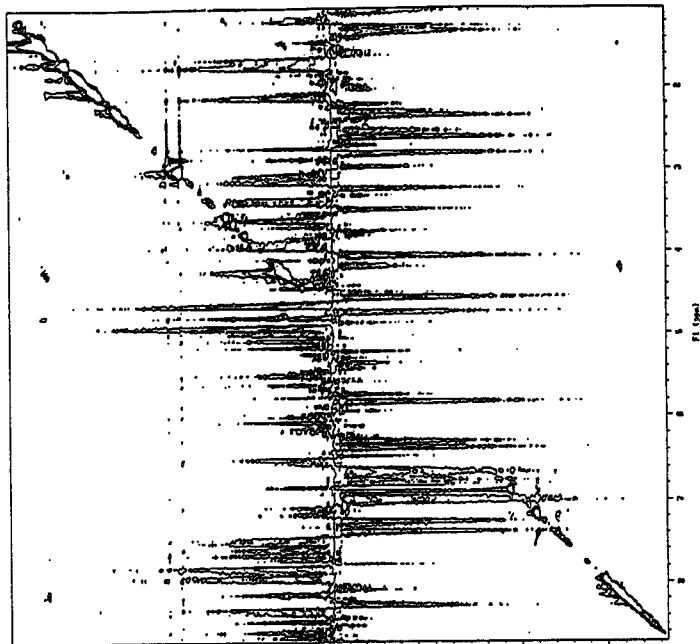
SSB16: 0
 SSB17: 0
 SSB18: 0
 SSB19: 0
 SSB20: 0



Appendix 4.2.2 EK3.3 1H 1-D Spectrum at pH 5.5 200MHz

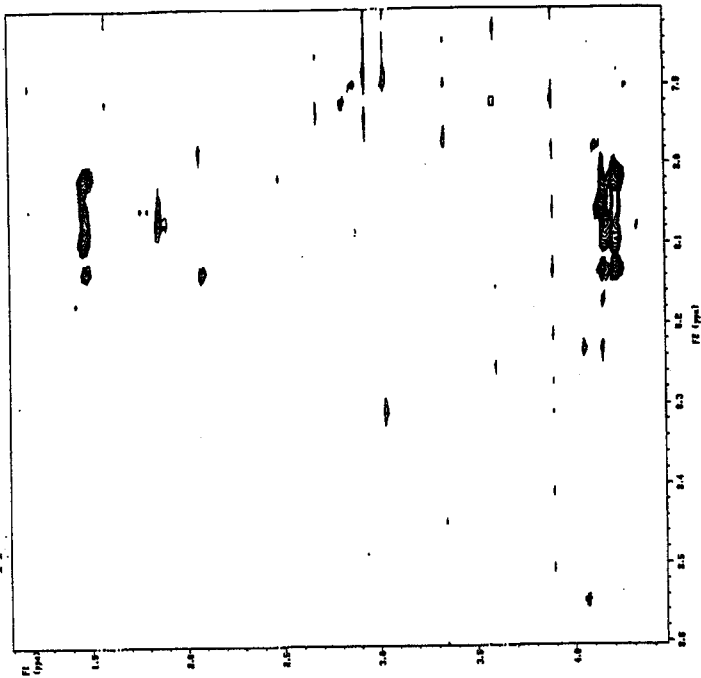


Appendix 4.4 EK4.0 NOESY pH5.5 200 ms mixing time



NAME:
 Date:
 Run:
 Operator:
 Sample:
 CONCENTRATION:
 Solute:
 Solvent:
 pH:
 Temp:
 Acq:
 1.1:
 2.1:
 3.1:
 4.1:
 5.1:
 6.1:
 7.1:
 8.1:
 9.1:
 10.1:
 11.1:
 12.1:
 13.1:
 14.1:
 15.1:
 16.1:
 17.1:
 18.1:
 19.1:
 20.1:
 21.1:
 22.1:
 23.1:
 24.1:
 25.1:
 26.1:
 27.1:
 28.1:
 29.1:
 30.1:
 31.1:
 32.1:
 33.1:
 34.1:
 35.1:
 36.1:
 37.1:
 38.1:
 39.1:
 40.1:
 41.1:
 42.1:
 43.1:
 44.1:
 45.1:
 46.1:
 47.1:
 48.1:
 49.1:
 50.1:
 51.1:
 52.1:
 53.1:
 54.1:
 55.1:
 56.1:
 57.1:
 58.1:
 59.1:
 60.1:
 61.1:
 62.1:
 63.1:
 64.1:
 65.1:
 66.1:
 67.1:
 68.1:
 69.1:
 70.1:
 71.1:
 72.1:
 73.1:
 74.1:
 75.1:
 76.1:
 77.1:
 78.1:
 79.1:
 80.1:
 81.1:
 82.1:
 83.1:
 84.1:
 85.1:
 86.1:
 87.1:
 88.1:
 89.1:
 90.1:
 91.1:
 92.1:
 93.1:
 94.1:
 95.1:
 96.1:
 97.1:
 98.1:
 99.1:
 100.1:

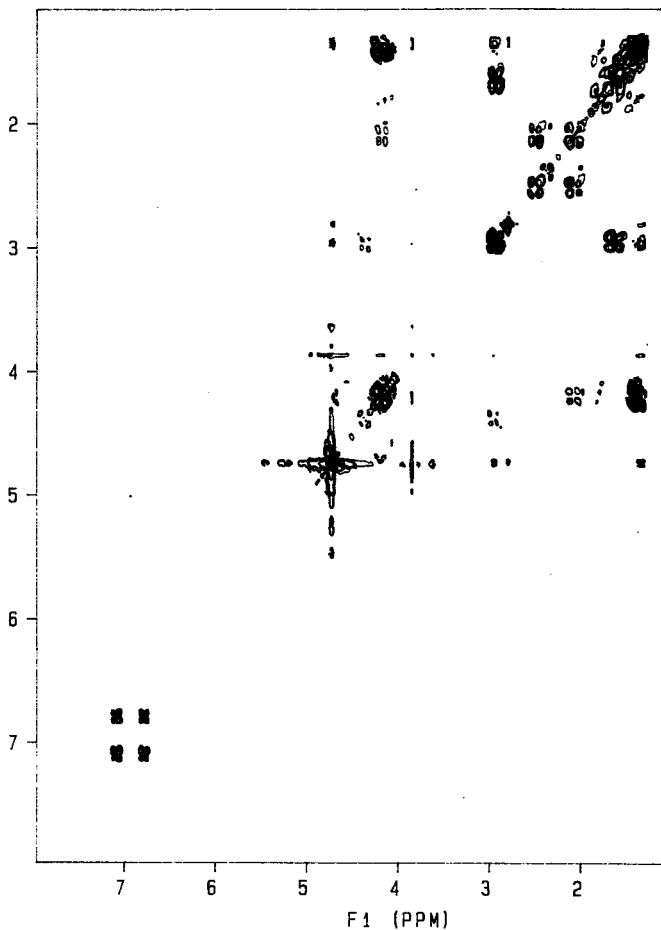
Appendix 4.6 EK3.3 NOESY pH5.5 200 ms mixing time



```

SAMPLE      NO. & W
-----
Acq  Per 01 41
P1  100  100
P2  100  100
P3  100  100
P4  100  100
P5  100  100
P6  100  100
P7  100  100
P8  100  100
P9  100  100
P10 100  100
P11 100  100
P12 100  100
P13 100  100
P14 100  100
P15 100  100
P16 100  100
P17 100  100
P18 100  100
P19 100  100
P20 100  100
P21 100  100
P22 100  100
P23 100  100
P24 100  100
P25 100  100
P26 100  100
P27 100  100
P28 100  100
P29 100  100
P30 100  100
P31 100  100
P32 100  100
P33 100  100
P34 100  100
P35 100  100
P36 100  100
P37 100  100
P38 100  100
P39 100  100
P40 100  100
P41 100  100
P42 100  100
P43 100  100
P44 100  100
P45 100  100
P46 100  100
P47 100  100
P48 100  100
P49 100  100
P50 100  100
P51 100  100
P52 100  100
P53 100  100
P54 100  100
P55 100  100
P56 100  100
P57 100  100
P58 100  100
P59 100  100
P60 100  100
P61 100  100
P62 100  100
P63 100  100
P64 100  100
P65 100  100
P66 100  100
P67 100  100
P68 100  100
P69 100  100
P70 100  100
P71 100  100
P72 100  100
P73 100  100
P74 100  100
P75 100  100
P76 100  100
P77 100  100
P78 100  100
P79 100  100
P80 100  100
P81 100  100
P82 100  100
P83 100  100
P84 100  100
P85 100  100
P86 100  100
P87 100  100
P88 100  100
P89 100  100
P90 100  100
P91 100  100
P92 100  100
P93 100  100
P94 100  100
P95 100  100
P96 100  100
P97 100  100
P98 100  100
P99 100  100
P100 100 100
  
```

F2 (PPM) Appendix 4.7.1 EK3.3 DQF-COSY pD 7.0 200MHz



F2 (PPM)

Appendix 4.7.2 EK3.3 DQF-COSY pD 7.0 200MHz
Expanded Region

